

*Large Hadron Collider Project*

**LHC Project Report 1163**

## **Conceptual Design of the LHC Interaction Region Upgrade – Phase-I**

V. Baglin, A. Ballarino, F. Cerutti, R. Denz, P. Fessia, K. Foraz, M. Fuerstner, W. Herr,  
M. Karppinen, N. Kos, H. Mainaud-Durand, A. Mereghetti, Y. Muttoni, D. Nisbet,  
R. Ostojic, H. Prin, J-P. Tock, R. van Weelderen, E. Wildner, L. Williams

Editors: R. Ostojic, L. Williams

### **Summary**

The LHC is starting operation with beam. The primary goal of CERN and the LHC community is to ensure that the collider is operated efficiently and that it achieves nominal performance in the shortest term. Since several years the community has been discussing the directions for maximizing the physics reach of the LHC by upgrading the experiments, in particular ATLAS and CMS, the LHC machine and the CERN proton injector complex, in a phased approach. The first phase of the LHC interaction region upgrade was approved by Council in December 2007. This phase relies on the mature Nb-Ti superconducting magnet technology with the target of increasing the LHC luminosity to 2 to 3  $10^{34} \text{ cm}^{-2}\text{s}^{-1}$ , while maximising the use of the existing infrastructure. In this report, we present the goals and the proposed conceptual solutions for the LHC IR Upgrade Phase-I which include the recommendations of the conceptual design review.

LHC-PROJECT-REPORT-1163  
12 Nov 2008



CERN – LHC Unit

CERN  
CH - 1211 Geneva 23  
Switzerland

Geneva, 12 Nov 2008



# Contents

<b>1. Goals and constraints of the Phase-I Upgrade .....</b>	<b>5</b>
<b>2. Layout and optics .....</b>	<b>6</b>
<b>3. Magnets.....</b>	<b>9</b>
3.1. Low- $\beta$ quadrupole .....	9
3.2. Correctors.....	13
3.3. D1 separation dipole .....	15
3.4. Cryostats and interconnections .....	16
<b>4. Cryogenic system .....</b>	<b>18</b>
4.1. Design constraints .....	18
4.2. Cooling of the triplets and correctors.....	19
4.3. Beam-screen cooling.....	20
4.4. D1 cooling options.....	20
<b>5. Powering and protection .....</b>	<b>21</b>
5.1. Powering options and converters .....	21
5.2. Magnet and circuit protection .....	24
5.3. Cold power transfer system .....	25
<b>6. Protection from particle debris .....</b>	<b>27</b>
6.1. Energy deposition and heat load in the magnets.....	27
6.2. Expected dose and equipment lifetime .....	30
6.3. TAS and TAN absorbers.....	31
6.4. Shielding of equipment areas .....	32
6.5. Radiation protection.....	33
<b>7. Vacuum system .....</b>	<b>34</b>
7.1. Vacuum system in the triplets.....	34
<b>8. Triplet alignment system .....</b>	<b>36</b>
8.1. Metrology of the assembled cryo-magnets .....	36
8.2. Initial alignment .....	36
8.3. Final alignment and stability.....	37
<b>9. Tunnel integration .....</b>	<b>38</b>
<b>10. Project organization and planning .....</b>	<b>40</b>
<b>11. References.....</b>	<b>42</b>



## 1. Goals and constraints of the Phase-I Upgrade

The LHC is ready for beam. By mid-2008, all of the machine sectors have been cooled down and the commissioning activities have almost been completed. The LHC construction effort has been considerable and has involved important international participation. In parallel with its construction, the HEP and accelerator communities have been discussing possible directions for increasing the scientific reach of this unique facility. The adopted approach, given in the strategy document of CERN Council [1], requires that any modifications in the LHC in the first years of running must comply with the operations schedule and the existing infrastructure. On the other hand, LHC relies on the existing injector chain and its reliability. These accelerators, in particular the PS, must have high priority in maintenance and upgrade. These considerations have lead to a phased approach to the upgrade of the LHC accelerator complex [2], which includes, in the first phase (2008-2013), the construction of a 160 MeV  $H^-$  proton linac (Linac4) and the Phase-I Upgrade of the LHC interaction regions.

The goal of the Phase-I Upgrade is to enable focusing of the beams to  $\beta^*$  of 0.25 m and reliable operation at a luminosity of 2 to 3  $10^{34} \text{ cm}^{-2}\text{s}^{-1}$ . The upgrade concerns in the first place the low- $\beta$  triplets in the two high-luminosity experiments, ATLAS and CMS, and assumes the same interface boundaries with the experiments as at present (located at 19 m on either side of the IP). The low- $\beta$  quadrupoles will feature a wider aperture than the present ones and will use the technology of Nb-Ti Rutherford-type cables cooled at 1.9 K developed for the LHC dipoles. The D1 separation dipoles, as well as a number of other elements in the insertions will also be modified so as to comply with a larger beam envelope associated with  $\beta^*$  of 0.25 m. However, the present cooling capacity of the cryogenic system and the other main infrastructure will remain unchanged, and will ultimately limit the luminosity reach of the upgrade.

The low- $\beta$  triplets presently installed in the LHC, shown in Figure 1, were built by a collaboration of CERN, Fermilab, KEK and LBNL [3]. The quadrupoles have a coil aperture of 70 mm, use Nb-Ti superconductor cables, and provide an operating gradient of 205 T/m. The 1.9 K cooling, electrical powering and all protection and control signals are fed to the triplet by an in-line feed-box. The triplets are positioned at  $L^*=23$  m from the interaction point (IP), and allow a  $\beta^*$  of 55 cm which corresponds to the nominal LHC luminosity of  $10^{34} \text{ cm}^{-2}\text{s}^{-1}$ .

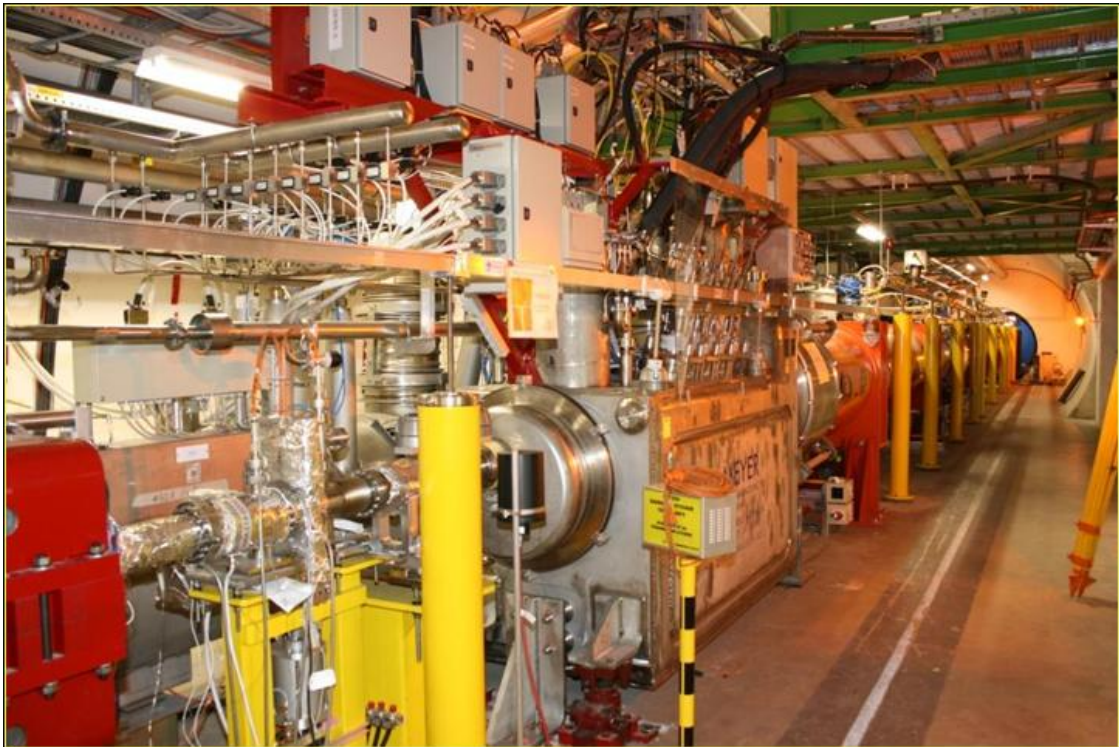


Figure 1: The low- $\beta$  triplet in the ATLAS interaction region.

The most effective way of reducing  $\beta^*$  is to reduce the distance of the triplet to the IP. Several studies have been made for the nominal LHC to arrange the various beam vacuum and alignment equipment housed in between the experimental area (19 m) and the triplet, with the purpose of reducing  $L^*$ . Unfortunately, the space for this equipment is extremely tight, inside heavy shielding and with limited access. In spite of considerable effort, it was not possible to bring the triplets forward, towards the IP, while maintaining the agreed upon interfaces between the experiments and the LHC machine.

The cryogenic power is brought to the triplets in ATLAS and CMS insertions by the compound cryo-line (QRL) from the cryogenic islands located in the LHC even points [4]. Since they are at the extremity of the QRL, the total cooling power available for the triplets will depend on the as-built heat loads in the adjacent arcs, which will be known better only after the first runs of the LHC with high-intensity beams. In any case, the total power available for each triplet cannot exceed 500 W at 1.9 K, which is the maximum power the sub-cooler installed in the QRL can provide. It should be noted that at present the cooling capacity available for the triplet in Sector 4-5 (left of CMS) is smaller than for the others as the RF cavities in IR4 use about 4 kW of the total capacity of the cryo-plant servicing this sector (23 kW at 4.5-20 K). Also, the present sectorization of the QRL does not allow to warm-up the insertion magnets separately from the arcs. Hence, four LHC sectors have to be warmed-up to exchange the triplets in ATLAS and CMS insertions.

It is clear that any increase of cooling requirements, in particular those related to the increase of luminosity above  $2$  to  $3 \cdot 10^{34} \text{ cm}^{-2}\text{s}^{-1}$  will need dedicated cryogenic plants serving the triplets around ATLAS and CMS. Their installation will most likely require a certain level of civil engineering in the underground areas. These changes are best done at the time of the phase-II upgrade when the two experiments will also perform their own extensive modifications.

As shown in Figure 1, all major equipment of the triplets is located in the LHC tunnel, with the exception of the power converters which are housed in the UJ alcoves adjacent to the machine tunnel in ATLAS, and the USC alcove parallel to the experimental cavern in CMS. The alcoves are separated from the tunnel by shielding walls, through which water-cooled cables pass and link the power converters to the triplet feed-boxes. Access for maintenance of the equipment in the tunnel, in particular of the feed-boxes, is difficult and may have consequences on scheduling of the LHC operation. In view of the even higher radiation levels after the Phase-I Upgrade, it is necessary to remove all delicate equipment from the tunnel, including the feed-boxes, and place it in low radiation areas. Such areas are very scarce around the ATLAS and CMS triplets, and it may be necessary to further shield the alcoves.

The access and transport of magnets to and from ATLAS and CMS implies long hauls over several kilometres alongside the chain of cold LHC magnets. Although care had been taken during LHC design to enable transport of magnets at any time, the LHC tunnel is tight and transport of equipment is a delicate operation. Preparing the triplets for transport therefore has to be carefully planned. It is also clear that all new equipment has to comply with the allowed transport envelope, which coincides with the length, cross-section and mass of the LHC main cryo-dipole.

It is well known from the optics and beam studies made during the LHC design that a reduction of  $\beta^*$ , while directly leading to the luminosity increase, has a number of important consequences on the performance of the machine. The chromatic aberrations, linear and of higher order, are particularly serious and must be carefully controlled and compensated. Of particular concern is the off-momentum beta-beating,  $\Delta\beta(\delta)/\beta(0)$ , which must be compensated in the triplets and in the betatron and momentum cleaning insertions (IR7 and IR3). It should be noted that  $\Delta\beta(\delta)/\beta(0)$  larger than about 10% may corrupt the collimation system [5]. As chromatic aberrations concern the LHC as a whole, new optics solutions need to be examined for the Phase-I Upgrade while using the existing corrector circuits to their maximum potential.

## 2. Layout and optics

The present LHC low- $\beta$  triplet, shown in Figure 2, is of the symmetric type with the two outboard magnets, Q1 and Q3, with a magnetic length of 6.6 m, while the two inner magnets, Q2A and Q2B (forming a single cold mass Q2), have a length of 5.7 m. The interconnect lengths between Q1-Q2 and Q2-Q3 are slightly different. The orbit and other correctors are distributed in all three cryo-magnets. The separation dipole D1 is composed of six modules of normal conducting magnets. The DFBX feed-box is placed in the beam line, in between the triplet and the D1 dipole. In IR1 and IR5, the triplet is separated from the matching section by a drift space of about 70 m [4].

The present matching sections comprise stand-alone superconducting magnets (D2-Q6) separated by warm sections, which contain the collimators, beam instrumentation and vacuum equipment, as well as elements of the energy extraction system for the main dipole circuits in the adjacent arcs. The area is also used for forward physics experiments that need direct access to the beam-line. An example of the complexity

of the equipment is shown in Figure 3 for the section between the TAN and D2 dipole. Most of this equipment will remain in service after the Phase-I Upgrade.

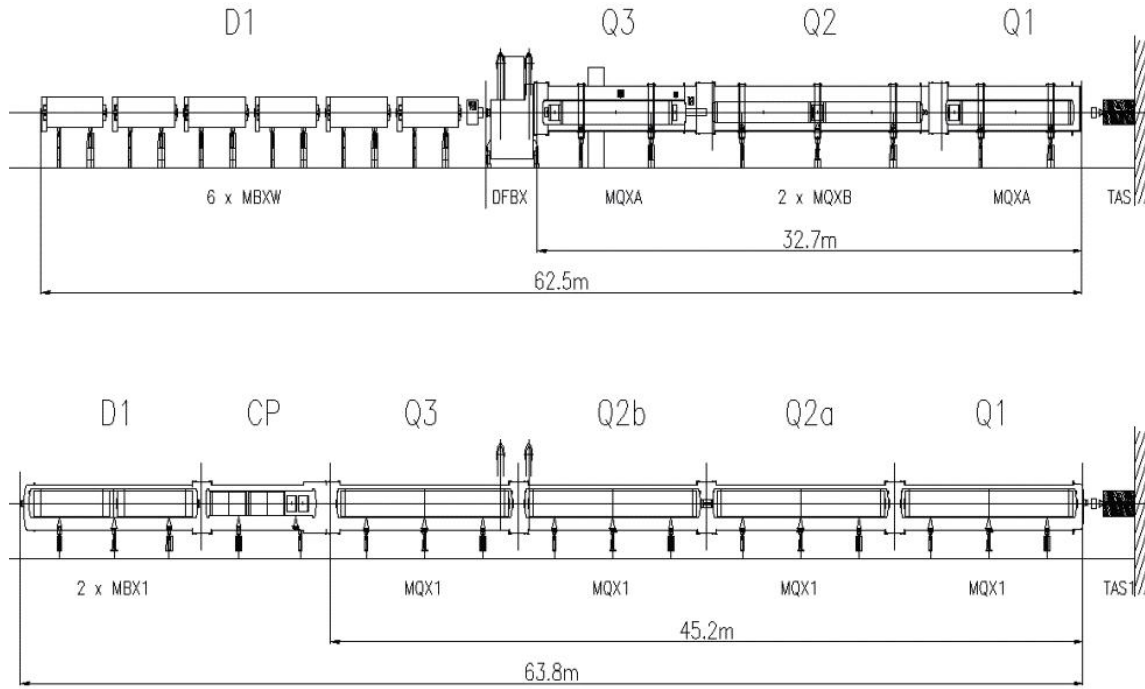


Figure 2: Layout of the present LHC triplet (top) and the proposed layout of the triplet for the Phase-I Upgrade (bottom)

The magnets in the matching section are cooled in a saturated helium bath at 4.5 K and are powered through a superconducting link which is about 120 m long. Studies made during the LHC design have determined that a change of their operating temperature to 1.9 K is technically very difficult due to the limited size of the QRL “jumpers” and increased number of connections to the headers that would be required in this case. In the arcs, these connections are distributed over several cells. The increase of the strength or of the temperature margin of the magnets by cooling them to 1.9 K is therefore not possible without extensive modifications of the QRL. Modification of the beam screens in these magnets requires their warm-up and removal from the tunnel, while their relocation to new positions implies considerable intervention on the cryo-services (QRL and superconducting link), and displacement of the cabling and power services in the tunnel. For all these reasons it has been decided that the design of the insertions for the Phase-I Upgrade should proceed assuming that the matching section magnets and their operating margins remain unchanged.

Reduction of  $\beta^*$  inevitably leads to tighter aperture in the matching section magnets and nearby equipment. Protection against the beam halo, which is at present assured by tertiary collimators designed to protect the triplets, will most likely need to be extended to other magnets as well. In addition, the TAN will require extensive modifications to handle the higher debris power and provide appropriate aperture for the beams. The new protection equipment and other interventions in the matching sections (e.g. realignment of the critical warm elements) will be done during normal shutdown periods for the LHC, foreseen at the beginning of every calendar year. The design of the new equipment must take into account the implications on the background in the experiments, which is expected to be an important issue for high-luminosity runs of the LHC.

The triplet for the Phase-I Upgrade will necessarily be longer than the present one, as the operating gradient that can be provided by the Nb-Ti conductor reduces with coil aperture. Nevertheless, the intention is to follow the symmetric layout as much as possible, as it offers a number of important advantages. A preliminary layout is shown in Figure 2, and features four identical magnets, each about 10 m long. The interconnections are also assumed to be identical. There are clear advantages of having identical magnets for their timely and cost-effective production. For similar reasons, it is proposed to group the corrector magnets in a separate cryo-unit placed on the upstream side of the triplet. Finally, a superconducting D1 dipole replaces the present normal conducting magnets, such that the full length of the new triplet string is almost identical to the present one.





Figure 3: Beam instrumentation, collimators and other equipment presently installed in between the TAN (red object on the left) and the D2 separation dipole (blue cryostat on the right) in the ATLAS matching section.

The Phase-I Upgrade requires a new optics solution for the LHC which minimizes chromatic aberrations. Such solutions, based on imposing a  $\pi/2$  betatron phase advance between IP1 and IP5, have been studied in the past for the nominal LHC, but without a fully satisfactory result. A new approach has been devised recently [6], which is based on using the sextupole families in the two sectors adjacent to each triplet to excite a  $\Delta\beta(\delta)$  wave that cancels the wave generated by the triplet. The solution requires that the phase advance in the arc cells is very close to  $\pi/2$  and that a well defined phase relation exists between the IP and the arc. Under these circumstances it has been shown that the problem of  $\Delta\beta(\delta)/\beta(0)$  compensation can be solved. Using the maximal current of the sextupole families, the off-momentum beta-beating can be reduced below 10% everywhere in the LHC for  $\beta^* \geq 0.25$  m. Furthermore, these phase conditions also enable compensation of the spurious dispersion in the ring, generated by the large crossing angle, proportional to  $1/\sqrt{\beta^*}$ . However, as these phase conditions have to be achieved in all the arcs and insertions, the integer tune of the LHC changes, and the tune split is reduced from 5 to 3. Further work is necessary to fully validate the proposed solution at injection, possibly including experimental machine studies in the LHC itself.

Besides the phase conditions imposed by the ring optics, the optics in the ATLAS and CMS insertions must be consistent with the parameters of the new triplets and the magnets in the matching sections (D2-Q4) and dispersion suppressors (Q7-Q11), and of the other equipment that will remain after the Phase-I Upgrade. This concerns in particular the strength and aperture of the magnets, and the aperture of the collimators and absorbers. Several possibilities were examined [6] and it was found that as a general rule the shorter the focusing length of the new triplet the larger is the aperture margin in the matching sections, but the lower the flexibility of matching to the arc. On the other hand, by displacing Q4 and Q5 quadrupoles towards the arc by 10-15 m, the aperture and matching conditions for a given triplet can be improved. The longest Nb-Ti triplet that can be matched to the rest of the insertion is about 40 m long, and is given by the available strength and aperture of the dispersion suppressor quadrupoles.

On the basis of these arguments it was concluded that the appropriate solution for the Phase-I Upgrade is a low- $\beta$  quadrupole with a coil aperture of 120 mm and an operating gradient of 120 T/m. A number of layout issues still need to be resolved for the new triplet. For example, the preliminary studies have shown that for realistic alignment of the quadrupoles the orbit correction with a pair of orbit dipoles, as shown in



Figure 2, results in a small residual orbit error and favourable strength requirements [7]. However, the control of the beam position at the IP requires further studies. The number and position of the BPMs also has to be defined, as well as the space necessary for linking the triplet to the QRL and the cold power buses. Also, a precise evaluation is needed of the performance gain that would be obtained if the two central quadrupoles Q2A and Q2B were of different length than the Q1 and Q3 quadrupoles, as is the case in the present triplet. These and other questions will be resolved as the technical design proceeds to completion.

### 3. Magnets

The magnets for the Phase-I Upgrade will extensively use the technological developments made for the LHC. Nevertheless, the design of the new magnets is not without concerns due to higher stored energy, forces and stresses, and increased heat loads and radiation dose.

#### 3.1. Low- $\beta$ quadrupole

In the interest of reducing the technical and schedule risks associated with the development of a new superconducting cable, the design of the low- $\beta$  quadrupoles (MQXC) for the LHC Phase-I Upgrade is based on using the existing LHC dipole cables. Furthermore, the design should profit as much as possible from the tooling recovered from the various LHC production lines, and from the components and raw materials that have remained from the production of LHC magnets.

##### 3.1.1. Available material, components and tooling

The following items designed and procured for the LHC will be re-used:

1. The Nb-Ti Rutherford-type cable. The cables used will be the LHC main dipole Cable-01 and Cable-02 [4]. The available unit length is 448 m for Cable-01 and 740 m for Cable-02, which allows production of a quadrupole with an aperture of up to 130 mm and a length of up to 11.5m. The full quantity of cable for manufacture of 20 low- $\beta$  quadrupoles is available at CERN.
2. Collar steel. A total of 136 t of YUS 130 austenitic steel in 3 mm thick sheets is available at CERN. This material, produced by Nippon Steel, has a thermal contraction coefficient from room temperature to 1.9 K of  $2.6 \cdot 10^{-3}$ . The available quantity is sufficient for manufacture of 20 low- $\beta$  collared coils.
3. Low carbon yoke steel. A total of 262 t of Magnetil, produced by Cockerill, is available at CERN in 5.8 mm thick sheets. This quantity is not sufficient for 20 cold masses and additional material needs to be purchased. As an alternative, purchase of 700 t required for the full production could also be considered, as it would allow uniformity of the yokes without mixing of the steel grades.
4. Tooling. Significant tooling has been retrieved from the various LHC production lines and will be installed or modified at CERN. Of particular interest are the winding machine, coil curing press and shell welding press. The welding press determines the maximum outer diameter of the cold mass of 570 mm (diameter of the LHC dipole).

All materials used, either existing or new ones, will be checked for compliance with the level of radiation expected in the triplets. The most critical in terms of the radiation dose are the insulating materials, in particular the G11 epoxy-glass used in the LHC magnets for the coil heads. An elemental trace analysis will be done for the steels and other materials so as to be able to predict the activation level of the cryo-magnets after exposure to the beam.

##### 3.1.2. Cable insulation

The cable insulation for the LHC dipoles uses polyimide tapes and has proven to be robust with excellent electrical and thermal properties [4]. As an alternative, and in view of higher heat loads, a new insulation topology has been proposed for the quadrupoles so as to increase its permeability to superfluid helium [8]. The scheme uses of 3 layers of polyimide tape, as shown in Figure 4:

- 1<sup>st</sup> layer: a 9 mm wide, 50  $\mu$ m thick tape, with a wrap spacing of 1 mm
- 2<sup>nd</sup> layer: a 3 mm wide, 50  $\mu$ m or 75  $\mu$ m thick tape, with a wrap spacing of 1.5 mm, counter wise to the 1<sup>st</sup> layer
- 3<sup>rd</sup> layer: a 9 mm wide, 69  $\mu$ m thick tape, with uncured polyimide glue on the outer surface. The glue is hardened during curing to provide mechanical stability and size of the coil.

In this scheme the electrical insulation is provided by the combined effect of the 1st and of 3rd layers, while the middle layer provides channels that enable heat transfer to the helium bath of the magnet. The insulation scheme is being thoroughly tested electrically, mechanically and thermally. The results of the first tests are very encouraging.

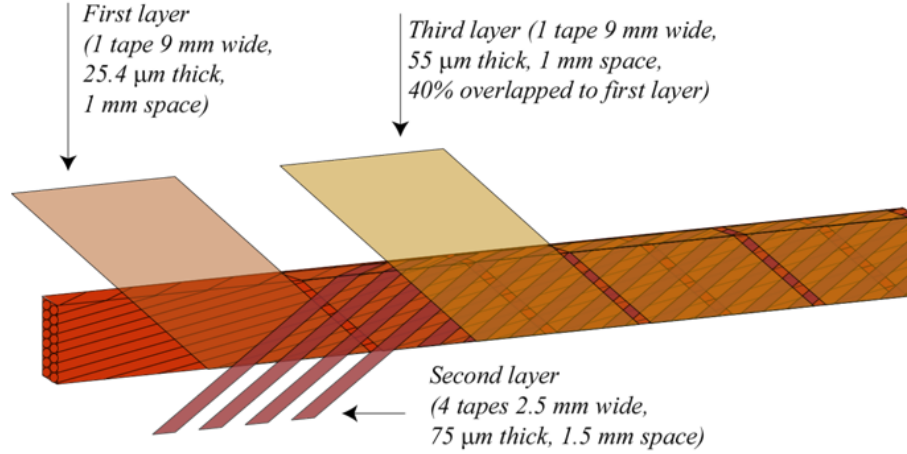


Figure 4: Cable insulation scheme proposed for the low- $\beta$  quadrupole.

### 3.1.3. Magnetic design

An extensive analysis [9] of possible coil configurations has been carried out in order to determine the maximum field gradient that can be achieved using the LHC superconducting cable. The configurations that have been selected, shown in Figure 5, have two layers, with Cable-01 in the inner layer and Cable-02 in the outer layer. For a coil aperture of 110 mm the maximum achievable short sample gradient is 160 T/m. For an aperture of 120 mm the maximum decreases to 149 T/m, and for 130 mm it is about 138 T/m. For the low- $\beta$  quadrupoles in the LHC, it is considered that the nominal working point should be around 80 % of the design maximum, which gives nominal operating gradients of 128 T/m for a 110 mm aperture, 119 T/m for a 120 mm aperture and 110 for a 130 mm aperture.

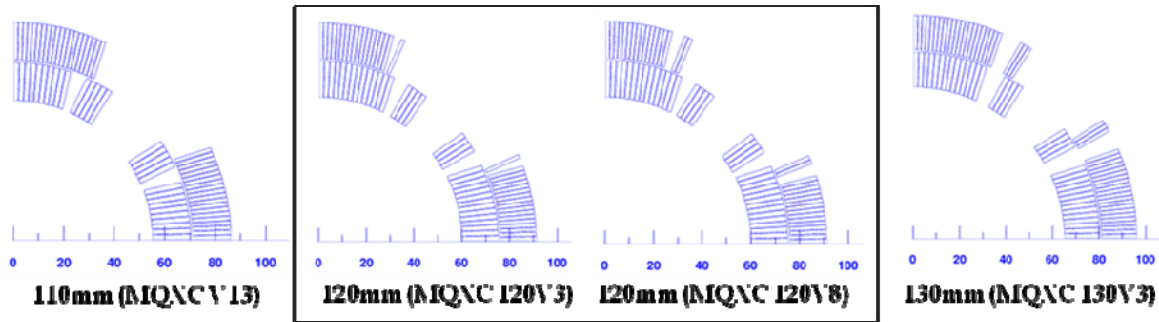


Figure 5: Possible conductor distributions for coil apertures of 110 mm, 120 mm and 130 mm.

Further analysis has been done for the preferred coil aperture of 120 mm. The angular dimension of the inner layer has been set to 40 degrees providing a transverse dimension of the innermost end spacer of 10 mm, which corresponds to the dimension of the spacer used in the LHC main dipole. Good quality and stability of the winding has been achieved with these spacers. The preferred coil layout, Figure 5, has four blocks (two in the inner and two in the outer layer), which provides sufficient parameters for tuning the field quality. Appropriate ground insulation will be provided between the poles and in the mid-plane, which could also be used to correct the field quality without modifying the coil and iron design.

As discussed in Section 4.2, an internal heat exchanger is the preferred solution for cooling the low- $\beta$  quadrupoles at 1.9 K. In this case two configurations are possible, with one 95 mm ID heat exchanger, or two

68 mm ID heat exchangers. In both cases, for reasons of symmetry, four holes need to be provided in the yoke, either located in line with the midplanes (one heat exchanger), or in line with the poles, at 45 degrees from the midplanes (one or two heat exchangers). The influence of the holes on the magnetic design is greater in the first case, but as shown in Figure 6 the reduction of the transfer function is between 0.2% and 0.5%, similar to that of the present low- $\beta$  quadrupoles (MQXA and MQXB). The impact of the holes on the field quality can be compensated by small adjustments of the coil design and by using additional features in the yoke design. A design with one heat exchanger, located in the upper mid-plane of the magnet as shown in Figure 7, is considered to be the best compromise as it leads to standardization of the magnets and of the interconnections between them.

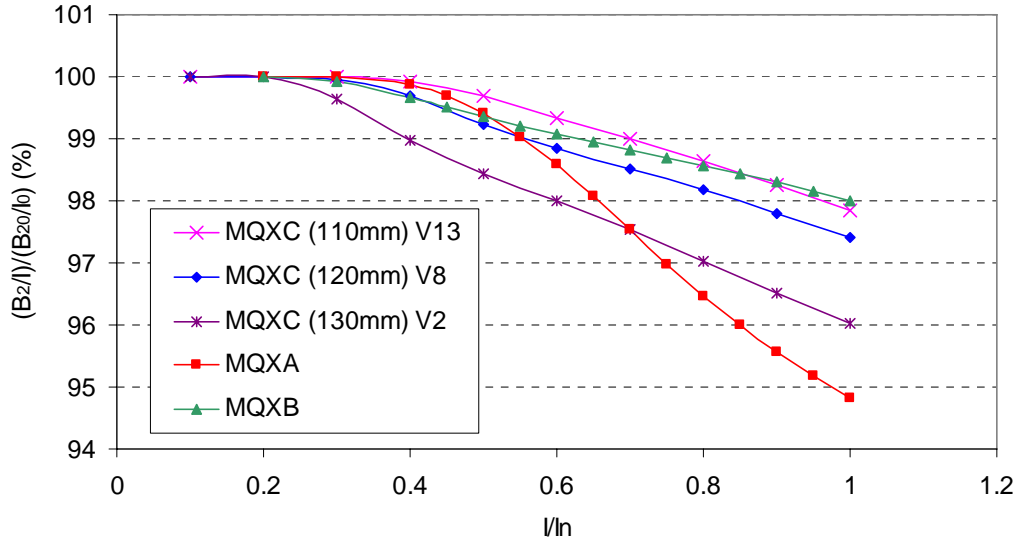


Figure 6: Normalised transfer functions of the present low- $\beta$  quadrupoles (MQXA and MQXB) and of three possible designs of MQXC (aperture 110, 120 and 130mm) with four 110 mm holes, one of which is used for the heat exchanger.

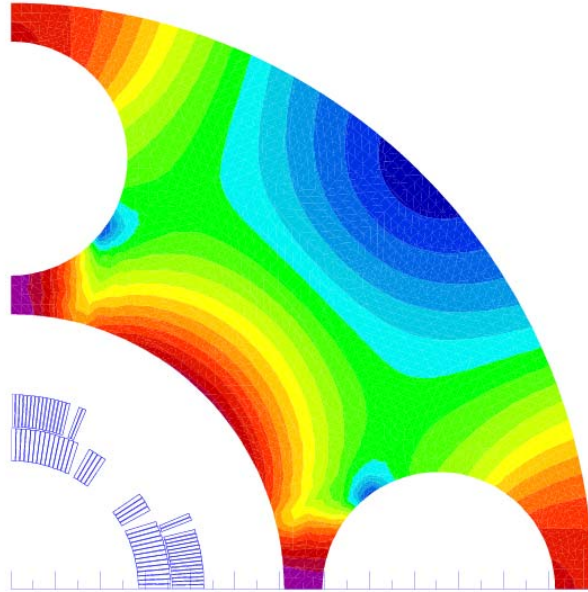


Figure 7: Conceptual design of the 120 mm MQXC quadrupole with a 110 mm opening for the heat exchanger.

### 3.1.4. Magnet protection

Several possibilities for protecting the magnets have been considered, taking into account considerable experience with the LHC dipole cables, quench heaters and their powering units, as well as with the external elements of the protection circuits. With this information at hand, several circuit configurations were analysed [10], as given in Figure 8.




Setup		Nominal Current		Half Current	
		T peak	MIITs	T peak	MIITs
Dump resistor 40 mOhm, 10 ms delay (electronics and switch)		117	33.6	--	--
	Q.H. over 11 cables	157	33.3	78	23.0
	Q.H. over 11 cables with an extra delay of 20 ms	157	36.4	78	23.7
	Only half of the heaters operational	220	38.1	103	27.5
	Q.H. over 2x4 cables	180	35.2	86	24.5
	Q.H. over 11 cables with an extra delay of 20 ms	217	38.0	104	27.6
	Only half of the heaters operational	221	43.4	102	30.8
	Q.H. over 11 cables + Dump Resistor	118	29.4	50	15.2
	Q.H. over 11 cables + Dump Resistor, Only half of the heaters operational	136	29.8	--	--

Figure 8: Main results of quench protection studies.

In summary:

- 1) A 40 mΩ dump resistor, limiting the peak voltage in the magnet to about 500 V, is extremely effective, as the peak temperature in the coil is less than 120 K.
- 2) Quench heaters covering 11 cables of the outer coil layer and wired in two independent circuits (two quench heaters per pole), result in a peak temperature of less than 160 K. In case of malfunction of one of the heater circuits the maximum temperature in the coil would be 220 K.
- 3) Subdivision of quench heaters, with four heating strips per pole, each covering 4 cables, provides an additional level of redundancy in case of circuit failure. However, there is a loss of total efficiency as the peak temperature is 180 K.
- 4) A 40 mΩ dump resistor together with quench heaters as in case (2) provides a high level of redundancy. The peak temperature is then less than 120 K, and increases to 136 K if only half of the heaters are activated.

The above results indicate that the magnet design is sound and that it can be effectively protected with any of the usual protection schemes. An external dump resistor, backed with quench heaters configured in two families, presents multiple advantages and has been retained as the baseline (Section 5).

### 3.1.5. Mechanical design

The estimated electromagnetic force in a 130 mm aperture MQXC quadrupole is 1.8 MN/m per quadrant, while the azimuthal stress on the mid-plane is of the order of 85 MPa. These values are higher than in any other LHC quadrupole, but are still in the range that can be contained by self supporting stainless steel

collars. This concept also has the advantage of decoupling the mechanical and magnetic design of the collared coils from the magnet yoke. An extensive study has been made to determine the parameters of the collars and their deformation under various loads [11]. A summary of the results obtained are given in Figure 9, where the displacement of the outer layer is shown as a function of the collar width. Clearly, a collar width of around 35 mm is necessary to limit coil displacement. A similar value is also obtained when considering the compressive stress at the pole of the inner layer and its variation with the bending of the collars. Assuming that the radial displacement of the coils in the mid-plane should satisfy the criteria defined for the other LHC quadrupoles (displacement less than 60  $\mu\text{m}$ ), we conclude that a collar 35 to 37 mm wide is best adapted for the 120 mm aperture quadrupole.

A locking system comprising eight keys is considered as the best compromise for the 260 to 270 mm outer collar diameter. Depending on their angular position, the force on the keys and the stiffness of the structure can be modified. The best solution was found when the keys are at 15 degrees from the mid plane, in which case the force on each key is about half of the total burst force, while the coil displacement due to collar bending is below 60  $\mu\text{m}$ .

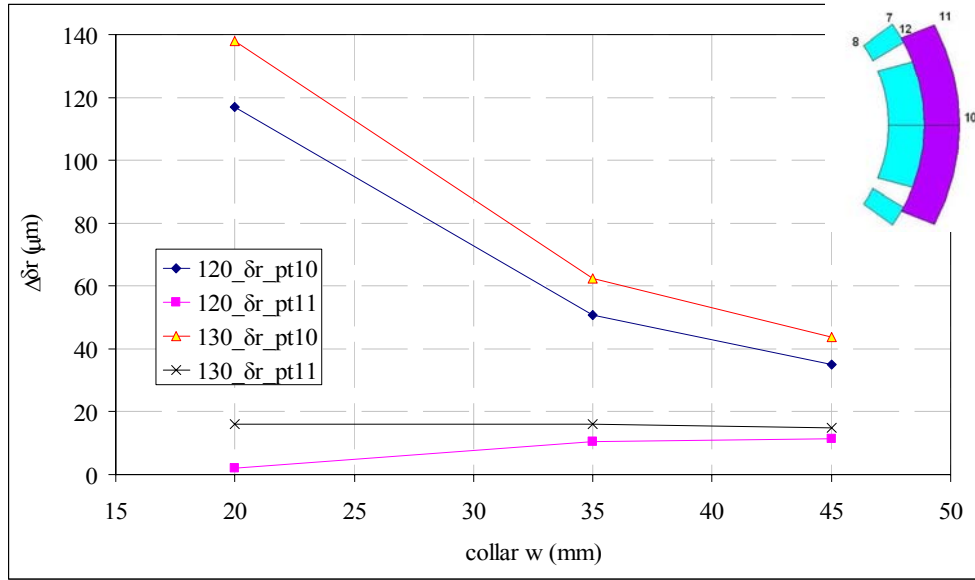


Figure 9: Radial coil displacement of the edges of the coil outer layer as function of the collar thickness.

The design of the magnet yoke and its helium vessel is presently envisaged to follow the design of the LHC insertion quadrupoles [4]. A single piece yoke will be used to provide the return path for the magnetic flux and magnetic shielding. The mechanical function of the yoke will be to align the collared coils, but otherwise it will not participate in containing the forces. The final alignment of the magnet will be provided by the full length shells, welded at the median plane. This technique has proven to be very reliable, giving excellent results in aligning the magnets. The helium vessel will be completed with end-domes, much in the style of the LHC dipoles.

### 3.2. Correctors

In the proposed layout the corrector magnets are grouped in a separate cryo-unit, located between Q3 and D1. The assembly is cooled in line with the triplet at 1.9 K, and will contain horizontal and vertical orbit correctors (MCBX), and skew quadrupole (MQSX) and sextupole (MCSX) correctors. Other multipole correctors may also be necessary. The required strength of the correctors will be determined on the basis of the field error tables for the low- $\beta$  quadrupoles and the D1 dipole. The corrector cryo-unit is expected to be about 6 m long. The aperture of the magnets will be compatible with the 120 mm aperture of the low- $\beta$  quadrupoles. The initial studies of the magnet protection from particle debris (Section 6.1) indicate that a larger aperture would allow reduction of the power density, which could be further reduced by adding shielding between the beam tube and the coils. With this in mind, an aperture of 140 mm is being considered for all correctors.

### 3.2.1. MCBX

With respect to the present triplet, a smaller number of orbit correctors is proposed. Their strength is estimated at about 6 Tm. These magnets will also provide the crossing angle for the beams and their separation at the IP before collision. Hence, they should be constructed with the same level of reliability and robustness in mind as any other dipole in the LHC. The nested dipole correctors based on epoxy-impregnated coils, as used in the present triplet, are not considered appropriate for the performance goals of the Phase-I Upgrade and alternative solutions using Rutherford-type cables are being investigated. Besides helium transparency, this type of coil should also profit from the larger temperature margin offered by 1.9 K cooling. However, their design requires careful optimization and must include the full powering circuit, in particular the power converter. Contrary to the present rating of 600 A, bipolar powering in the 2 to 3 kA range will be necessary. In addition, an active quench protection system will be required for these magnets. Similarly, the mechanical design should profit from the experience with the LHC magnets using stand-alone collars. Development work on the cables, preferably using existing strands, and on the design of the magnet and the converter, as well as circuit protection, has been launched to meet these goals. A preliminary design is shown in Figure 10.

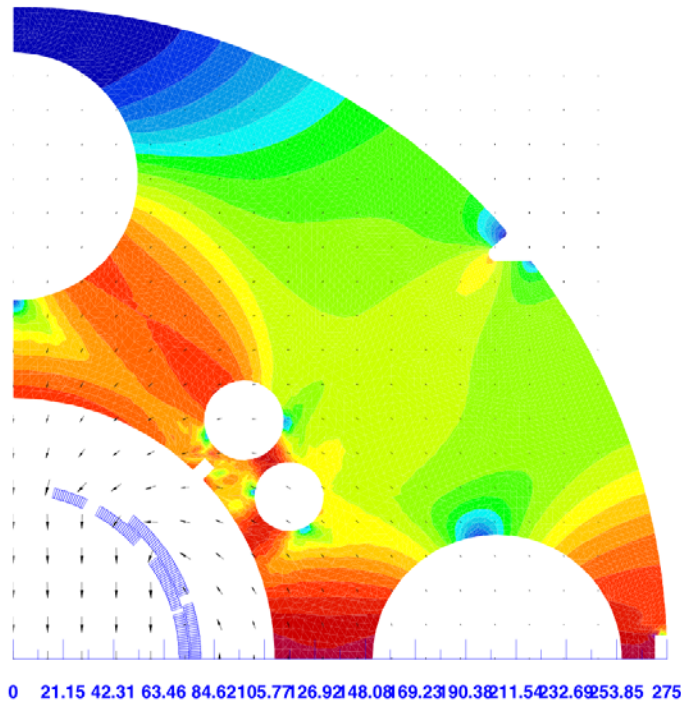


Figure 10: Conceptual design of a high-current dipole corrector MCBX.

### 3.2.2. MQSX

Two design options have been considered for the skew quadrupoles: a low-current version based on epoxy-impregnated coils and a mechanical structure similar to the magnets installed in the present triplet, and a high-current version based on a small Rutherford-type cable. The coils in the low-current version are made by counter-winding the existing 0.73 x 1.25 mm superconducting wire used in the LHC correctors [4], pre-assembled in a 3-wire cable. The windings are connected in series by ultra-sonic welding at the end plate. The main concern with such a coil is the low radiation hardness of the wire insulation. This type of winding also requires a large operating margin, typically in the range of 40 to 60 %. The clamping structure could be based on off-centred laminations compressed with a shrinking cylinder, as in the present magnets.

The high-current version would use a small Rutherford type cable, similar to that considered for the MCBX magnet, and a collar-key structure. This solution would require a powering system capable of delivering around 1.5 kA. A preliminary design is shown in Figure 11.



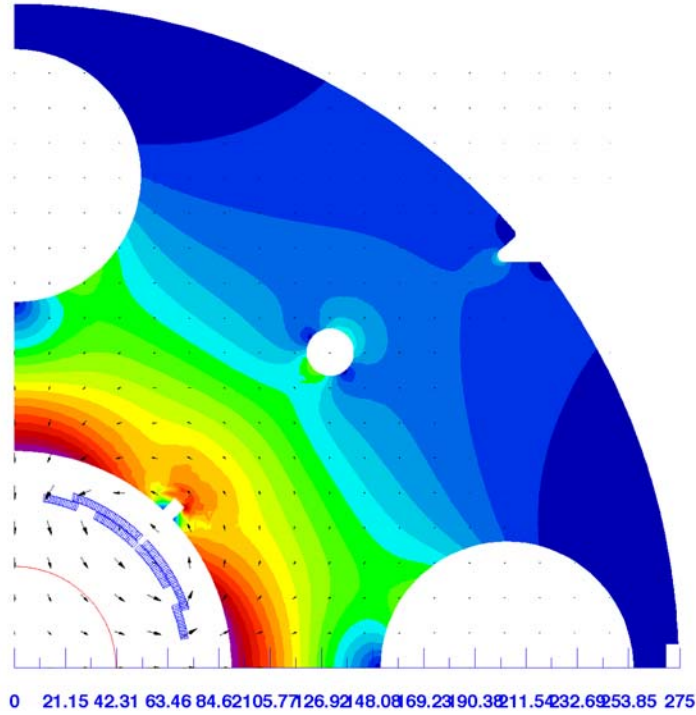


Figure 11: Conceptual design of a high-current skew-quadrupole corrector MQSX.

### 3.2.3. MCSX

On the basis of the preliminary estimates of the required strength for the sextupole corrector, similar to the present one, a super-ferric magnet could be an interesting alternative. This design would also offer additional advantages as the simple racetrack coils are located relatively far from the beam. The mechanical structure is also very simple. The epoxy-impregnated coils could be wound with a single wire, so that a low current, in the range of 50 A to 100 A, would be needed. Such a magnet would not require any active quench protection.

### 3.3. D1 separation dipole

The present D1 separation dipole comprises six normal conducting magnets with a pole gap of 63 mm. Clearly, the magnet gap must be increased to match the aperture of the new triplet. Recent technical analysis and cost estimates have determined that the most effective solution for the D1 dipole is a superconducting magnet with a field in the 4 T range.

The preferred solution for the superconducting D1 dipoles is to reuse the design of the DX dipole, which has been serving well in RHIC for many years. This magnet has a coil aperture of 180 mm with a warm bore of 140 mm [12], as shown in Figure 12. The operating field of the magnet is 4.4 T and its magnetic length 3.7 m. Two such magnets are necessary for D1, which will be about 10 m long, as shown in Figure 2. The magnet will be cooled at 4.5 K and could be either a semi- or a fully stand-alone unit (with a warm bore). The parameters of the magnet are such that it could remain in the insertions for the phase-II upgrade.

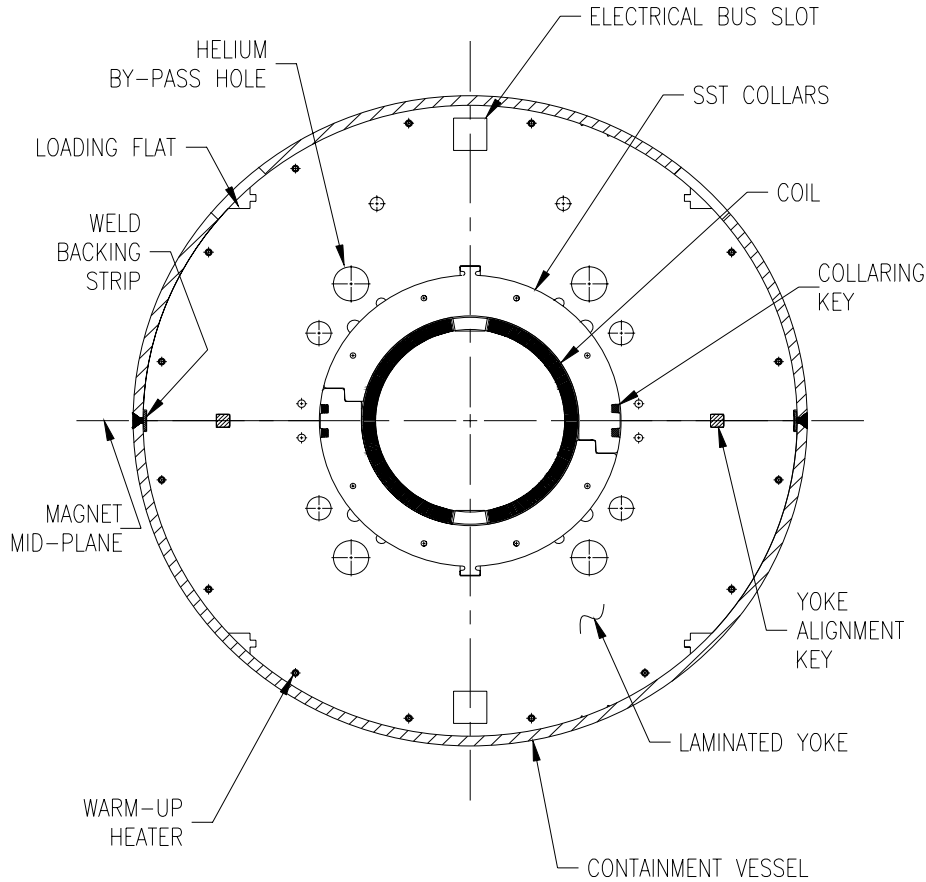


Figure 12: Cross-section of the RHIC DX magnet.

### 3.4. Cryostats and interconnections

#### 3.4.1. Cryostats

The cryostat is required to stably support the cold mass with respect to the ground and precisely position it with respect to the beam axis. Furthermore, it should thermally insulate the cold mass from the ambient surroundings, thus enabling it to be cooled to operating temperature and maintained there at reasonable operating cost. The cryostat components for the Phase-I Upgrade magnets will be identical to or very close derivatives of those currently in use in the LHC [4]. The thermal performance of these components has been measured and the results are well documented. The principal characteristics of the components are summarized as follows.

##### *Support posts*

The support posts provide precise positioning of the cold masses within their cryostats. The load-bearing part is composed of a monolithic 4 mm thick tubular column in Glass Fibre Reinforced Epoxy composite material (GFRE) chosen for its low thermal conductivity-to-stiffness ratio. Each support post is equipped with two aluminium heat intercept plates and with stainless steel internal rings, glued to the composite column. They are conduction cooled at 4.5-10 K and 50-70 K via two cryogenic lines. The positioning repeatability of the cold mass, when subjected to variable forces, is defined by the dispersion of stiffness characteristics of the composite columns. The thermal contraction of the columns, during operational temperature variations, will also have certain dispersion. For these reasons, a strict material and manufacturing process quality control will be implemented.

Each quadrupole will be internally supported on either 2 or 3 support posts. Further studies of the performance of the two options, as well as the analysis of the required tooling, will be performed. The corrector cryo-unit will be supported on two support posts.

### ***Thermal shield and radiation screen***

The thermal shield assembly is composed of a lower double-walled tray formed from two extruded half-profiles in series 6060 aluminium alloy welded together, and a series of upper shells clipped into place and welded to the lower tray. Welding is used to keep thermal impedance low and maximise the heat extraction from the thermal shield assembly to the cold source. The lower tray incorporates two tubular channels, which are used as cryogenic lines for the passage of the cold gaseous helium at a temperature of about 50-70 K and pressure of up to 20 bars to which heat is extracted from the thermal shield assembly and the support posts. At each end of the cryogenic lines, industrially available aluminium-alloy-to-stainless-steel pipe transition elements are welded on. Stainless steel welding can then be employed on all interconnect pipe-work to be assembled in the tunnel. To minimise radiative heat transfer, the thermal shield is wrapped with 2 Multilayer Insulation (MLI) blankets each made up of 15 layers of aluminised Mylar and 14 spacer layers.

The radiation screen consists of a MLI blanket made up of 10 layers of aluminised Mylar and 9 spacer layers. This blanket is wrapped around the cold mass to help maintain adequate cryostat thermal insulation under conditions of degraded vacuum. The radiation screen is not actively cooled. The inside and outside temperatures will therefore float to intermediate values between those of the cold mass and the thermal shield.

### ***Vacuum vessel***

The vacuum vessel minimises convective heat transfer and provides a precise and stable in time support to the cold mass. It will consist of a long cylindrical tube with end flanges in AISI 304L for vacuum tight connection via elastomeric or metallic seals to adjacent units.

The vacuum vessel dimensions, outer diameter 914 mm (36 inches) and wall thickness 12 mm, are based on those of industrial standard tubes manufactured in alloyed low carbon steel. Vessels fabricated entirely from alloyed low carbon steel plate rolled to form are also an acceptable option. In case of a cryogenic leak, the pressure can rise to 0.14 MPa absolute. In addition to this pressure rise, rapid local cooling of the vessel wall to about 230 K may occur. The steel selected for the vacuum vessel wall must demonstrate adequate energy absorption during a standard Charpy test at -50 °C.

The support regions are designed such that the planes of internal support (cold mass to vacuum vessel) and external support to ground are coincident. Load is shared through circumferential reinforcement rings. Reinforcing angles will be supplied on the vessel top surface to support alignment fixtures. ISO standard flanged ports for vacuum pumping and relief, and the passage of diagnostics and controls will be located azimuthally in the wall of the vessel. The dimensional stability of the finished vacuum vessels with the passage of time is particularly important. Stress relieving probably by vibration techniques will be required.

### ***External support to ground***

Each cryo-magnet assembly is supported to ground via specifically designed jacks. Their function is to hold the cryo-magnet in a known position while withstanding forces occurring during all phases of normal operation, and to allow positioning of the cryo-magnet along all three orthogonal axes to be adjusted using external fiducials. This adjustment will be possible over the range and within the precision specified for the alignment system, by hand and also by remote means using electric motors and control equipment suitably hardened for use in a radioactive environment

### ***3.4.2. Interconnections***

Once in their final position in the tunnel, the new magnets have to be interconnected between themselves and to the QRL and the superconducting link to ensure continuity of the beam vacuum, electrical continuity of the bus-bars for powering the magnets, and of the insulation vacuum and the cryogenic lines (cold mass helium enclosure, heat exchanger, thermal shield and beam screen cooling, etc.). The interconnections have to provide the mechanical compensation due to thermal shrinkage of the neighbouring components and allow smooth and unrestricted movement of the cryo-magnets required for their realignment once in operating conditions.

The interconnections will be executed in the tunnel activated by several years of LHC operation before the Phase-I Upgrade. Furthermore, in view of the possible consolidation activities and in particular of the phase-II upgrade, the interconnections will need to be dismantled in a highly radioactive environment (Section 6.5). This aspect must be taken into account from the design phase, by maximising the use of automatic (possibly remotely operated) tooling, minimising the duration of in-situ interventions, and by taking precautions to minimise generation of waste.

The technologies used for the LHC interconnections will be the basis for the new ones. For the beam vacuum and the cryogenics lines, orbital TIG welding will be used, avoiding manual welding wherever

possible. This technique proved to be very efficient and reliable, and meets all requirements of mechanical resistance and leak tightness. As the Nb-Ti cable is the same as for the LHC dipole, the electrical connections will be made by joining the cable and the copper stabilizer by adding a Sn-Ag strip in between. The soldering will be executed under pressure to ensure low electrical resistance. Two heat sources are possible: resistive or inductive soldering. The choice will be made based on the available space. The continuity of the radiative screen will be ensured in the interconnections by appropriate supports and a specific MLI blanket. The actively cooled thermal shield will be made of aluminium covered by MLI. The insulation vacuum enclosure will be closed by stainless steel bellows, identical to the ones used in the LHC.

In order to ensure the quality of the interconnections, several inspections and tests will be carried out in the workshops and in-situ in the tunnel. As done for LHC, the welding procedures will be qualified in the workshops, and weld samples regularly tested for mechanical properties and leak tightness. All tooling and welders will be qualified as part of the standard CERN procedures. All welds executed in the tunnel will be qualified by independent inspectors, leak tests and X-rays, wherever possible. The final assembly will be pressure and leak tested. The electrical joints will be qualified on samples by ultrasonic inspection, electrical tests at cryogenic temperature and mechanical tests both at room and cryogenic temperature. Extensive electrical tests will be done at each stage during tunnel execution.

## 4. Cryogenic system

### 4.1. Design constraints

The cooling of the magnets for the Phase-I Upgrade and the associated cold power transfer system will be realized within the boundaries of the existing cryogenic infrastructure: the types and maximum available quantities of cryogens may not exceed the presently available supply provided in IR1 and IR5 by the cryogenic distribution line (QRL) and the respective refrigeration systems [4]. Design pressures of the new equipment are also subject to the present LHC specification [13]. As a consequence, the maximum superfluid helium cooling capacity available is 500 W for each triplet (including the correctors), corresponding to the maximum capacity of the counterflow sub-cooler installed in the QRL service module. The exact capacity could be somewhat less than 500 W, depending on the actual integrated consumption of each of the four LHC sectors which contain the triplets in IR1 and IR5. Similarly, the temperatures and pressures of the supply and return headers in the QRL vary slightly from their nominal values in every insertion [14]. Sub-coolers for helium supply from header C (nominal pressure 3.6 bar and nominal temperature 4.6 K) should therefore be considered if a stable inlet temperature is required. The pressure of header D should be considered to be in the range of  $130 \text{ kPa} \pm 25 \text{ kPa}$ , which corresponds to the saturated vapour temperature of  $4.5 \text{ K} \pm 0.2 \text{ K}$  for the equipment cooled by pool boiling.

The present QRL service modules contain most of the functionalities necessary for the Phase-I Upgrade and the aim is to reuse them in order to limit the costs. Increasing the piping dimension is not possible, but within reasonable limits the existing valves can be adapted to new requirements by changing their poppets. Functionalities exceeding the possibilities of the existing service module would need to be provided by a local cryogenic distribution box. The QRL service module itself could remain in its present location and the new magnets and local cryogenic distribution box fed by a dedicated cryogenic extension line. It seems, however, for reasons of minimizing pressure losses and due to limited tunnel space, that it is more advantageous to move them closer to the new interface location in between the correctors and D1. In this case, the construction of entirely new service modules should also be considered.

The estimated heat loads considered for the main circuits are given in Table 1. Unless stated explicitly, a contingency factor of  $1.25 \times 1.5 = 1.875$  is used to take into account the uncertainties in estimating the static and dynamic loads.

Table 1: Heat loads in the main cooling circuits

Cooling circuit	T level (K)	Heat load (W)	Heat load with contingency (W)	Comment
Triplet and corrector cold masses	1.9	500	500	Chosen design limit, Contingency factor 1.0
Triplet and corrector beam screen	4.5 – 20	106	212	2 W/m over 52.9 m, Contingency factor 2.0
D1 cold mass [15]	4.5 – 6	42	79	10 W (static), 20 W (dynamic), 12 W (warm bore) Standard contingency allows for warm bore bake-out
Thermal screens	50 – 70	500	500	Average 8 W/m, Contingency factor 1.0
Cold power transfer link: cables and DFX	4.5 – 6	24	45	0.4 W/m, 60 m length
Cold power transfer link: thermal screen	6 – 20 or 50 – 70	240	450	4 W/m, 60 m length

#### 4.2. Cooling of the triplets and correctors

The quadrupoles and the correctors will be cooled in pressurized static superfluid helium bath at 1.3 bar and at a temperature of about 1.9 K. For thermal design purposes, a total length of the string of 52.9 m (Figure 2), an average heat load of 9.5 W/m and localized peaks of up to 30 W/m (Section 6.1), and a total heat load of 500 W are assumed.

The heat generated in the magnets will be extracted by vaporization of superfluid helium which travels as a low pressure two-phase flow in a bayonet heat exchanger [16], which can be installed either external to the cold masses, as in the present triplets, or located in the magnet yokes as in the regular LHC arc magnets. The low vapour pressure inside the heat exchanger is maintained by a cold compressor system, with a suction pressure of 15 mbar, corresponding to the saturation temperature of 1.776 K. The cold compressor system is located in the LHC even points, 3.3 km away from the triplets, connected via the QRL [4]. The maximum temperature difference between the magnets and the cold compressor is 2.17 K ( $T_\lambda$ )-1.776 K = 394 mK. This is reduced by about 92 mK due to the pressure drop in the QRL, and by another 10 mK in the counterflow heat exchanger in the QRL service module. The available temperature difference for the Phase-I triplet is therefore 292 mK.

The bayonet heat exchanger consists of a smooth copper tube, with adequate wall thickness to comply with the design pressure in the cold masses of 20 bar. The copper conductivity at 1.9 K should be at least 1000 W/Km, so that the temperature drop across the copper wall remains negligible compared to the Kapitza resistance. It was shown that at vapour velocities of 5 m/s some liquid droplets get into the vapour stream, and that at 7 m/s the functioning of the heat exchanger is disrupted by the amount of liquid in the flow and the associated pressure increase [16, 17]. The size of the heat exchanger is determined by the maximum vapour velocity of 7 m/s and the total available heat exchange area, when it is wetted over its full length. Of the two criteria, the vapour velocity limit is the more stringent and is met if the inner diameter of the heat exchanger is greater than 95 mm. Two parallel exchangers with 68 mm ID could equally be used, but the preference is for a single heat exchanger.

Assuming an average wetted perimeter fraction in the heat exchanger of 16.4 %, copper conductivity of 1000 W/Km and Kapitza resistance of 914 T<sup>3</sup> W/(m<sup>2</sup> K), the calculated heat exchange capacity of this heat exchanger is 143 W/Km. At full length wetting and for 500 W extracted power, this leads to a temperature drop across the heat exchanger wall of 66 mK, to which additional 11 mK have to be added due to the pressure drop, giving a total of 77 mK. Due to the tunnel slope, an additional pumping line is required within the triplet cryostat to return the vapour to the low pressure header of the QRL. In order not to further increase the saturation temperature for heat exchange its inner diameter should be at least 100 mm. This will add another 14 mK at 500 W. Therefore, the bath temperature in the triplets is 1.969 K at 500 W thermal load. The temperature profile in the system is summarised in Table 2.

Table 2: Saturation temperature in the cooling system for the Phase-I triplet at 500 W thermal load (95 mm ID bayonet heat exchanger and 100 mm ID pumping line).

Location	T (K)	Available $\Delta T$ to $T_\lambda$ (mK)
cold compressor station	1.776	394
cold compressor station - HX outlet (3.3 km QRL)	1.868	302
HX outlet - HX inlet	1.878	292
HX inlet – bayonet HX outlet (52.9 m pumping line)	1.892	278
Superfluid bath in the triplet	1.969	201

With the magnet bath at 1.969 K, any additional temperature drop from the coils to the heat exchanger should be minimised. The conduction path is shortest, only radial, with an internal heat exchanger. For an external one, the heat would first have to be transported radially to a location with sufficient free helium cross-section, then longitudinally to the magnet interconnects and then again further alongside the heat exchanger. This would require a considerable free helium volume for longitudinal transport and an additional temperature drop of about 20 mK. As the quadrupole symmetry requires four holes in the yoke laminations (Figure 7), three free holes of about 200 cm<sup>2</sup> total area are sufficient for temperature regulation in case of the internal heat exchanger and also provide the required hydraulic cross-section for helium gas flow in transient conditions. This option is also a good compromise for the magnets and interconnections, and is therefore considered as the baseline. Attention should be given as well to the yoke and collar packing so as to maximize the effectiveness of the heat transport to the internal heat exchanger.

### 4.3. Beam-screen cooling

A beam-screen is foreseen in the quadrupoles and correctors (Section 7.1) and will be actively cooled with supercritical helium in the temperature range of 5-20 K, as is presently done in all LHC beam screens [4]. Because of the considerably higher expected heat load (2 W/m) than at present, the possibility of cooling the beam screen in the range of 40-60 K was also considered, but was found to be of little interest [18]. The supercritical helium is supplied from header C at 2.5 bar and returned to header D at 1.3 bar. With 0.5 bar reserved for the temperature regulated flow control valve, 0.7 bar remains for dimensioning the beam-screen cooling tubes. The best compromise is then to use four standard LHC cooling tubes (3.7 mm ID), cooled in parallel, which then allows a factor of two contingency with respect to the estimated heat load.

### 4.4. D1 cooling options

The preferred solution for the superconducting D1 dipoles (Section 3.3) is to use the design of the DX dipole, which is cooled in RHIC by forced flow of supercritical helium at 4.6 K [12]. In LHC, this magnet can be either cooled by pool boiling helium or by forced flow of supercritical helium. In both cases the supply will come from QRL header C and the return will go to QRL header D.

In pool boiling helium the magnet operating temperature will be determined by the QRL header D pressure of 130 kPa  $\pm$  25 kPa, which corresponds to a saturation temperature of 4.5 K  $\pm$  0.2 K. This is a proven configuration for the LHC insertion magnets and has the lowest helium consumption. Therefore, we consider this as the reference configuration.

The DX magnet in RHIC is part of a string of magnets cooled by the flow of supercritical helium, which acts as transport medium, absorbing heat in the magnets and then rejecting it to a bath of pool boiling helium via re-coolers. The cooling capacity is determined by the size of the re-coolers, whereas the heat exchange efficiency in the magnets is determined by the mass flow of supercritical helium. Since the two functionalities are effectively decoupled by the separate supercritical and pool boiling helium circuits, low temperature gradients along the magnets can be achieved by using a high enough supercritical flow rate, and appropriately dimensioned re-coolers.

Cooling of D1 with supercritical helium in the LHC can be achieved by taking the supply from QRL header C and returning the flow via a flow-control valve to header D. In this open-loop scheme it is not possible to achieve a low-temperature gradient along D1 with a mass flow comparable to the pool boiling configuration. With 42 W heat load and mass flow of about 7 g/s a temperature gradient across D1 is expected to be about 1.5 K, whereas pool boiling at 4.5 K requires 2.6 g/s with zero temperature gradient across D1. Only with supercritical flows of about 100 g/s can the temperature gradient be limited to 0.1 K.



Alternatively, a closed-loop system with a cold re-circulator capable of 100 g/s could be considered and its performance compared to the reference configuration in terms of operating margin for the magnet and efficiency of helium usage.

## 5. Powering and protection

### 5.1. Powering options and converters

#### 5.1.1. Triplet quadrupole circuits

The choice of powering topology for the main quadrupole circuits should first consider the nominal LHC triplet powering topology. The nominal LHC design required that a large difference in operating current between Q2 and Q1/3 be accommodated, and that the volume of equipment installed underground be minimised. The adopted solution was a topology that nested 3 converters together. While this works well, several systems are inductively coupled, introducing complexity to the control and protection electronics. As such, the final commissioning of the triplet systems has also been complex. With this in mind, the objective for the upgrade should be to provide the powering flexibility while simplifying the topology where possible. It is also assumed that, contrary to the present triplet, the upgrade will make use of an energy extraction system.

Several options were considered for the powering scheme.

- Individual powering (Figure 11) – this option is the most flexible and straightforward implementation for powering. Each magnet has a dedicated power source, dimensioned for the nominal current. This allows the current in each magnet to be set arbitrarily to any level between the minimum and maximum value. However the solution demands the maximum volume for the powering equipment, as the nominal current must be installed in quadruplicate. Busbars and current leads would also be dimensioned for nominal current.

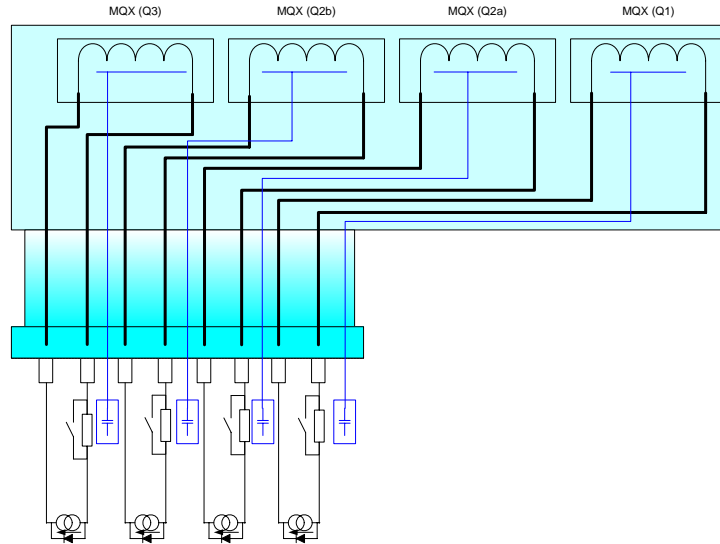


Figure 11: Individual powering electrical diagram.

- Nested powering (Figure 12) – a solution of this type would be very similar to that adopted for the present LHC triplet. A main converter circuit provides the high current source, with additional converters for current trimming in each magnet. Trim converters of either bipolar or unipolar current could be installed. Bipolar trims add complexity due to active protection being required, and the trim current is limited to a maximum of  $\pm 600$  A. Independent of the trim method, the protection of the circuits and the inductive decoupling of the currents is again required. The present experience shows this to be a complex solution, although the topology requires a minimal tunnel volume.

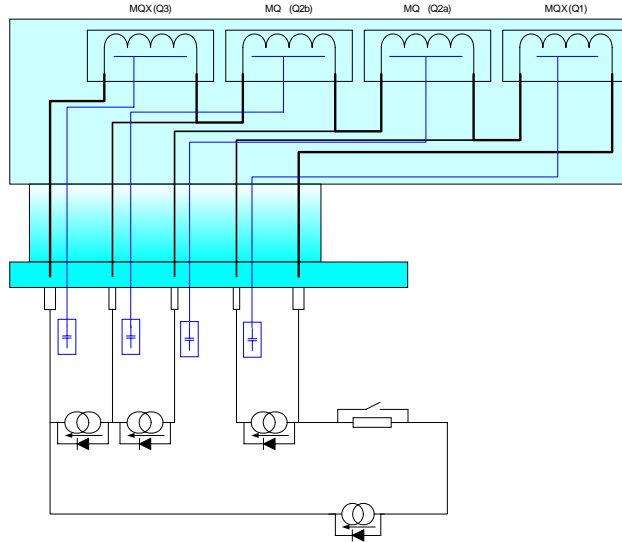


Figure 12: Nested powering electrical diagram.

- Split powering (Figure 13) – a compromise between fully nested and fully independent powering, this solution allows volume and cost to be optimised with only modest complexity. Magnets Q1 and Q2a are powered separately from Q2b and Q3. While inductive decoupling is still required, this is only necessary for two systems, which is relatively straightforward. The topology relies on the current difference between the magnets to be relatively small. At this time, the current difference is estimated to be approximately 2 kA. This also opens the possibility for optimisation of two of the current leads and busbars, which need to conduct only trim currents.

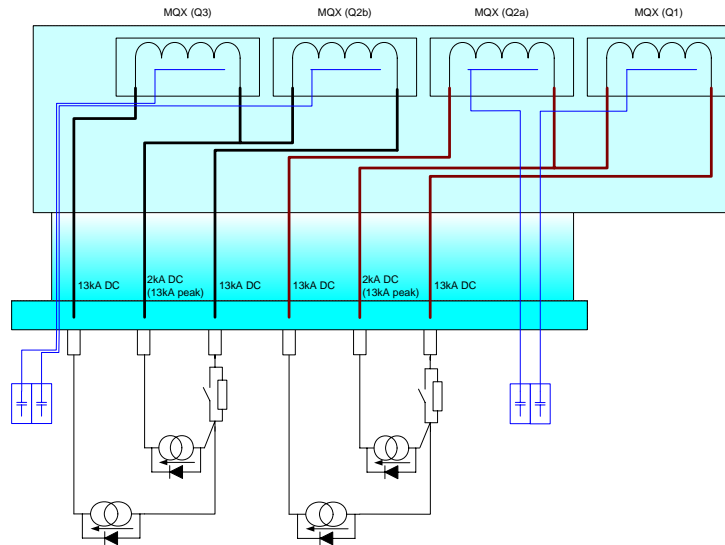


Figure 13: Split powering electrical diagram.

- Surface powering – radiation levels in the underground areas around the triplets is a major concern for LHC operation. Hence, the possibility of powering from the surface, where there are lesser volume constraints and no radiation constraints, should also be considered. An evaluation of a powering strategy from the surface indicates significant infrastructure and cost requirements, if the readily available copper DC cables are used. At Point 1, where this could be of most interest, new water cooled conductors would be required over several hundred meters. These would need to be installed in the main access shafts, with special reinforcement for the fixings, as the total weight would exceed 70 tonnes of copper. As a large amount of power would be required to compensate the resistive losses in the busbars, the surface cooling and electrical

infrastructure would also require to be modified. Conservative estimates for equipment costs of 5 MCHF and annual electrical costs of 1 MCHF, indicate this solution to be impractical. Other solutions, based on new superconducting materials (Section 5.3), are being considered and their use for connecting tunnel equipment with power converters located on the surface could be available for the phase-II upgrade.

After consideration of the above topological options, the split powering option was retained as the baseline. Certain performance limitations of the scheme remain to be validated. In particular, the controlled negative ramp rate capability of the circuit will be limited by the natural decay of the circuit, which will affect functions such as degaussing.

To meet the nominal current requirements, a primary current source of [14 kA, 8 V] is proposed. This would be implemented using several [2 kA, 8 V] sub-converter modules connected in parallel in an N+1 topology. The trim current source is proposed to be implemented as a 2 kA current source also with an N+1 topology. The system can be extended up to 4 kA nominal current in the future should the nominal trim current exceed 2 kA; however the redundancy offered by the N+1 topology would be lost. The main parameters of the converters and the circuits are summarized in Tables 3 and 4.

Table 3: Main quadrupole electrical circuit parameters

Parameter	Value
Power Converter Nominal Rating	[14 kA, 8 V]
Magnet Inductance (2 magnets)	104 mH
Maximum di/dt	10 A/s
DC Cable cross-section	2000 mm <sup>2</sup>
Maximum warm cable length	55 m (27.5 m per cable)
Minimum time constant	225 s
Power converter volume	6 x [19" x 2500 x 900 mm]

Table 4: Trim quadrupole electrical circuit parameters

Parameter	Value
Power Converter Nominal Rating	[2 kA, 8 V]
Magnet Inductance (1 magnet)	52 mH
Maximum di/dt	10 A/s
DC Cable cross-section	500 mm <sup>2</sup>
Maximum warm cable length	55 m (27.5 m per cable)
Minimum time constant	28 s
Power converter volume	2 x [19" x 2500 x 900 mm]

### 5.1.2. D1 separation dipole circuit

The D1 separation dipole is anticipated to be two RHIC DX magnets connected in series. The nominal operational current of the circuit is 5.6 kA; however currents up to 6.5 kA may be required. As such, a power converter rated [8 kA, 8 V] is proposed, using the same [2 kA, 8 V] power modules as those for the main quadrupole circuits. This system would be identical to those already powering the cold D1-D4 circuits in the LHC [4], with the exception that magnet energy extraction is planned to be used for the new circuits. The main parameters of the converters are summarized in Table 5.

Table 5: D1 Separation dipole electrical circuit parameters

Parameter	Value
Power Converter Nominal Rating	[8 kA, 8 V]
Magnet Inductance (2 magnets)	98 mH
Maximum di/dt	18 A/s
DC Cable cross-section	1300 mm <sup>2</sup>
Maximum warm cable length	60 m (30 m per cable)
Minimum time constant	126 s
Power converter volume	5 x [19" x 2500 x 900 mm]

### 5.1.3. Corrector circuits

Compared to the nominal LHC triplet layout, the Phase-I Upgrade anticipates fewer correctors. Where possible, the emphasis is on re-using existing LHC designs, in particular the [ $\pm 120$  A,  $\pm 10$  V] and [ $\pm 600$  A,  $\pm 10$  V] power converter families. However, due to concerns of radiation effects consideration is being given to designs based Rutherford-type superconducting cables and thus higher currents. The following represents tentative input for the circuit parameters:

- Dipole correctors (MCBXH/V) – a suitable magnet design using Rutherford-type cable would need a current of about 2500 A. Due to the functionality required, the power converter must be bipolar in current and voltage. A new power converter development is necessary to find a solution for this requirement. It is expected that energy extraction will be required for these circuits.
- Skew quadrupole corrector (MQSX) – preliminary studies suggest that a unipolar operating current of approximately 1500 A is required for a magnet design using a Rutherford-type cable. As such, it would be proposed to power this by a [2 kA, 8 V] power module; a new rack system is required for the converter modules. It is expected that energy extraction will be required for this circuit.
- Sextupole corrector (MCSX) - preliminary estimates suggest this circuit will operate with a bipolar current of between 50 A and 100 A, and as such can be powered by a [ $\pm 120$  A,  $\pm 10$  V] standard LHC power converter.

## 5.2. Magnet and circuit protection

Active protection systems will be required for the triplet quadrupoles, D1 dipole and high current corrector circuits. In all cases quench detection electronics for the magnets, bus-bars and the current leads as well as energy extraction systems will be required. The protection of the triplet quadrupoles and D1 will in addition make use of quench heaters.

### 5.2.1. Protection of the triplet quadrupoles

The present powering scheme for the triplets foresees grouping of the four magnets in two circuits, each with two nested power supplies and their current leads (Figure 13). The protection of the circuits will be very similar to that currently used for the LHC insertion quadrupoles, i.e. one detection system per magnet including the superconducting bus-bars and separate systems for the current leads. The protection parameters, like the thresholds and discrimination times, still need to be defined depending on the final magnet and circuit design. Tentative values are a detection threshold of  $U_{TH} = 100$  mV /  $t_{DIS} = 10$  ms for the circuit and the magnets and  $U_{TH} = 3$  mV /  $t_{DIS} = 100$  ms for the current leads.

The proposed powering scheme foresees one energy extraction system with 14 kA current rating per circuit, i.e. two per triplet. The cooling system of the extraction resistors must allow a sufficiently short cooling time after each extraction in order not to affect LHC operation. The magnets will also be equipped with two quench heater circuits each. Depending on its final location, the extraction system will be based either on mechanical circuit breakers or on semiconductor devices if the radiation levels in the installation area are sufficiently low. The peak voltage-to-ground will be 500-1000 V, depending on the chosen device technology.

### **5.2.2. Protection of D1 separation dipoles**

The protection system for the D1 dipole, which is assumed to comprise two magnets, will use an approach similar to that for the quadrupole circuits. Since the final configuration of the quench detection is not yet decided it is important that the bus-bars and the magnets are equipped with voltage taps, which will be used either for diagnostics or protection.

In addition to the energy extraction system with 6.5 kA current rating, quench heaters will also be used for protection. The present design is based on four heater circuits per D1 cryo-dipole. As for the quadrupole circuits there will be a dedicated protection system for the current leads and superconducting buses.

### **5.2.3. Protection of the correctors**

The protection of the correctors and the corresponding busbars will use a bridge based protection system similar to those currently employed for the protection of the LHC insertion quadrupoles. The bridge design will require a set of 2 x 3 redundant voltage taps. The midpoint voltage taps should be placed asymmetrically in order to allow an easy check of the magnet polarity. In addition there will be a dedicated protection system for the current leads, which may include also a part of the superconducting bus-bar, if needed.

While the correctors do not require quench heaters, it will be mandatory to use an energy extraction system with 2.5 kA current rating consisting of a circuit breaker and an extraction resistor.

### **5.2.4. Radiation tolerance**

It is preferable to install all quench detection electronics, data acquisition systems and quench heater discharge power supplies in areas not exposed to radiation. If the space and cabling constraints turn out to be such that the energy extraction systems, especially those for the triplet quadrupoles, have to be installed in radiation zones, then the design can only be based on mechanical circuit breakers.

### **5.2.5. Interfaces to LHC supervision and interlocks**

All protection electronics will be equipped with data acquisition systems communicating via a fieldbus link with the LHC control system. The quench detection systems will have hardwired links to the quench heater discharge power supplies, the energy extraction system and the corresponding powering interlock controller PIC. As for the LHC main circuits a discharge request for activating the energy extraction systems issued either by the power converter or the PIC can be implemented. The design of the data acquisition and interlock electronics and software will be based on existing LHC equipment and may require only moderate modifications.

### **5.2.6. Tests prior to installation**

After delivery all systems will undergo extensive individual testing at CERN. Based on the experience with LHC a string test is specifically regarded as very useful in order to check all interfaces and the compatibility with other systems.

## **5.3. Cold power transfer system**

With the increased level of radiation in the LHC tunnel expected in the Phase-I Upgrade, it is envisaged to place the current leads and their cryostats in a relatively radiation-free area near the power converters at some distance from the beam. The cold power transfer system therefore consists of the current leads, rated at the nominal current level of the magnet circuits, of a cryostat (DFX), incorporating the leads and providing the cryogens for their operation, and of a superconducting link, making the electrical connection between the magnets and the current leads. The use of a superconducting link brings a number of advantages [19], the most important of which is easier access to the system - cryostat and leads - which contains electrical devices that are sensitive to radiation (control valves, level gauges, ...), and need to be accessed for maintenance and electrical tests during the LHC shutdown periods. The routing of the link should conform to the general tunnel constraints (e.g. stay-clear zone for transport) and the mechanical limitations of the device itself, and should avoid as much as possible the areas exposed to radiation.

As an alternative to a conventional cold power transfer system incorporating a Nb-Ti bus, similar to the one presently used for powering the matching section magnets [4], a proposal based on the use of MgB<sub>2</sub> conductors has been studied [20]. The progress made in the last few years on this material is such that wires of about 1 mm diameter are today commercially available in long - kilometre - lengths with good homogeneity and electrical and mechanical properties that satisfy the requirements for this application. Recent measurements performed on wires of 1.1 mm diameter show a critical current of 436 A at 24 K in an

external field of 0.4 T [21]. The typical minimum bending diameter of the superconductor is about 100 times the diameter of the wire. The wire contains pre-reacted  $\text{MgB}_2$  filaments in a nickel and iron matrix. The filling factor is about 14 %. Copper stabilizer is incorporated in the inner core.

For the powering of the magnets in the Phase-I Upgrade, the proposal is to use  $\text{MgB}_2$  conductors at a maximum temperature of about 20 K. The concept is shown in Figure 14. The link is cooled by supercritical helium entering at 5 K on the magnet side, and reaching 15 -20 K at the lower end of the current leads, on the DFX side. The gas used for cooling of the link is also used for cooling of the leads and is recovered at room temperature. The flow of helium gas inside each lead is controlled by its temperature at the lower end, which will be maintained at 20 K. The cooling requirements are estimated to be such that in any operating conditions the mass flow through the leads guarantees sufficient cooling of the link.

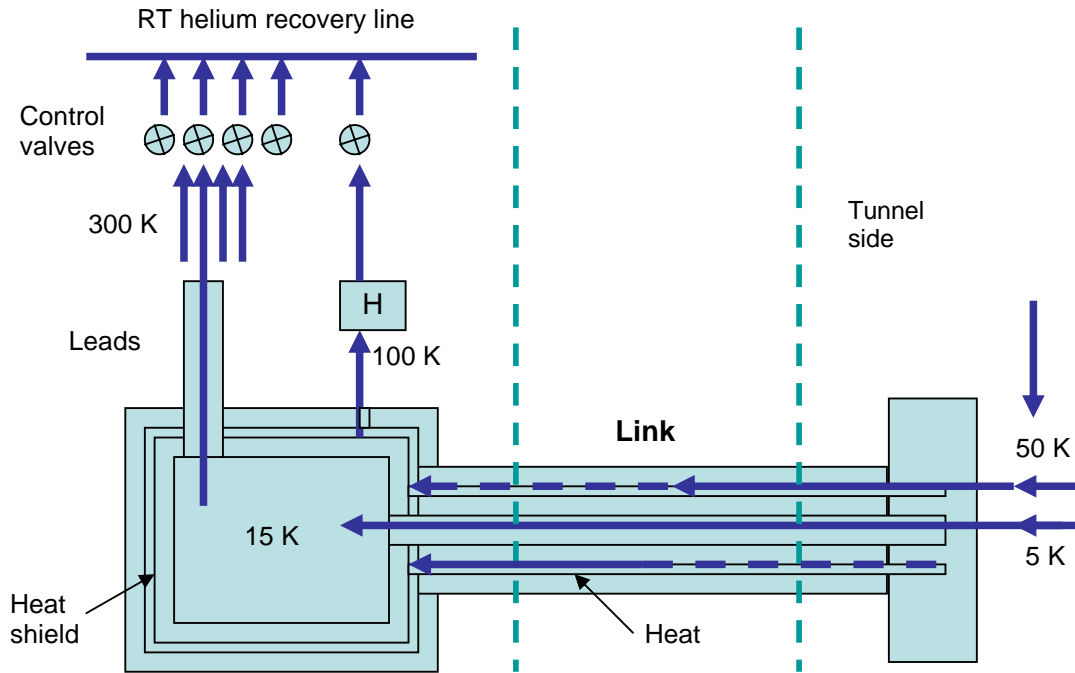


Figure 14: Concept of the cold power transfer system using  $\text{MgB}_2$  cable.

The proposed configuration of the link is based on the use of corrugated flexible pipes, which provide the vacuum insulation and the shielding via an actively helium-cooled thermal screen. The link contains all powering cables, which according to the present scheme includes six 14 kA cables for the quadrupoles and D1 dipole, six 2.5 kA cables for the trims and dipole correctors, and eight 0.6 kA cables for the other corrector magnets. Six multi-strand sub-cables, with an outer diameter of about 5.5 mm and a twist pitch of 300 mm, are assembled around an open helical tube to form an insulated and fully-transposed 14 kA conductor of about 18 mm external diameter. The 2.5 kA conductors are made of one sub-cable, while the 0.6 kA cables consist of three wires twisted together with stabilizing copper. The outer diameter of the multi-cable conductor is about 60 mm, while the outermost diameter of the vacuum envelope is about 200 mm. Instrumentation wires, mainly voltage taps required for protection of cables in case of resistive transition, are routed inside the link and extracted at the top of DFX.

The link will be assembled on the surface as a whole unit, up to about 60 meters long. The installation in the tunnel is conditioned by a minimum bending radius of about 2 meters. On the magnet side, the link will terminate with Nb-Ti wires already soldered to the  $\text{MgB}_2$  in an interconnection box attached to the link, which includes the  $\lambda$ -plate providing the separation between the supercritical helium of the link and the superfluid helium of the magnets. These Nb-Ti wires will be connected in the tunnel to the Nb-Ti buses installed in the magnets. On the DFX side, each cable of the link will be connected in-situ to the lower end of the leads.

In this concept, the leads are optimized and operated according to the same principles used for the LHC HTS high-current leads, with the  $\text{MgB}_2$  cable of the link replacing the Bi-2223 conductor of the lead. The leads are assembled on surface in their cryostat and transported to the tunnel.

The use of  $\text{MgB}_2$  link could also simplify the cryostat design: the cryostat does not need to be designed for liquid helium (with the related level control devices), since its cold mass would contain the helium gas



recovered from the link and conveyed through the leads. Compared to Nb-Ti link,  $\text{MgB}_2$  offers an important temperature margin, of the order of 10 K. Contrary to other HTS materials, e.g. Bi-2223 and Y-123 tapes, it can be drawn in the form of wires with isotropic electrical properties. Also,  $\text{MgB}_2$  is less costly than other commercially available HTS materials (Bi-2223, Bi-2212 and Y-123), and is well-suited for a power transfer link where the conductor operates in low magnetic field.

A study of an Nb-Ti link with associated conventional leads and cryostat is being made in parallel with the R&D activities aiming to demonstrate the feasibility of the  $\text{MgB}_2$  link. The final decision on the choice of the cable for the link will be taken at a later stage.

## 6. Protection from particle debris

With higher luminosities the protection of magnets and other equipment from particles generated in the collisions is of crucial importance. The starting point is to ensure that the magnets can sustain steady-state heat loads generated by the particle debris with adequate margin with respect to the quench limit. This issue has been studied in considerable detail for the present triplets and the coil protection was steadily improved until a factor of three safety margin with respect to estimated quench limits was achieved [22].

As the power density from the debris scales with luminosity, it is clear that the protection efficiency of the magnets in the Phase-I Upgrade must be higher than in the present triplet. It is assumed for the purposes of the conceptual design that the heat transfer properties of the new low- $\beta$  quadrupoles will be the same as in the present magnets, although work has started on improvements (Section 3.1). The same design limit for power density ( $4.3 \text{ mW/cm}^3$ ) is therefore assumed.

### 6.1. Energy deposition and heat load in the magnets

The energy deposition in the triplet depends on several parameters, notably on the distance from the collision point, triplet strength, aperture and length. A parametric study, based on the “symmetric” layout [23] and  $L^*$  of 23 m, gave important information on the energy deposition pattern and the margins that can be obtained [24]. The choice of apertures for this study and the resulting layouts are shown in Table 6. The aperture of the TAS was assumed 55 mm and the half crossing angle was  $225 \mu\text{rad}$ , in the vertical plane. The longitudinal separation between the magnets is an important parameter, as it defines the energy deposition at the entrance of the downstream magnet. The 1.3 m separation was taken, corresponding to the estimated minimum distance needed for interconnecting the magnets in the tunnel. The cold bore thickness was calculated to satisfy the pressure code requirements. The beam screen was 2 mm thick in all cases. The binning of the coil was chosen such to correspond to a minimum volume for equilibrium heat transport (width of the bin equal to the cable transverse dimensions, length equal to the twist pitch of the cable).

Table 6: The layout configurations in the parametric study of energy deposition in the new triplet.

Aperture (mm)	Gradient (T/m)	$L(Q1,Q3)$ (m)	$L(Q2a,b)$ (m)	Total length (m)
90	156	8.69	7.46	36.2
115	125	9.98	8.42	40.7
130	112	10.81	9.04	43.6
140	104	11.41	9.49	45.7

All the results presented in this section were obtained with the Monte Carlo code FLUKA [25, 26], relying on DPMJET3 as proton-proton event generator [27]. It has to be understood that although the results are given with good statistical errors (about 10% for peak power values and less than 1% for integral values), they carry significant systematic uncertainties related to the interaction/transport models, extrapolation of cross sections to 14 TeV centre-of-mass energy, geometry and material implementation, crucial dependence on a very small angular range of the reaction products, etc. Thus, a safety margin of a factor of three in peak power density is a necessary assumption for this kind of calculations.

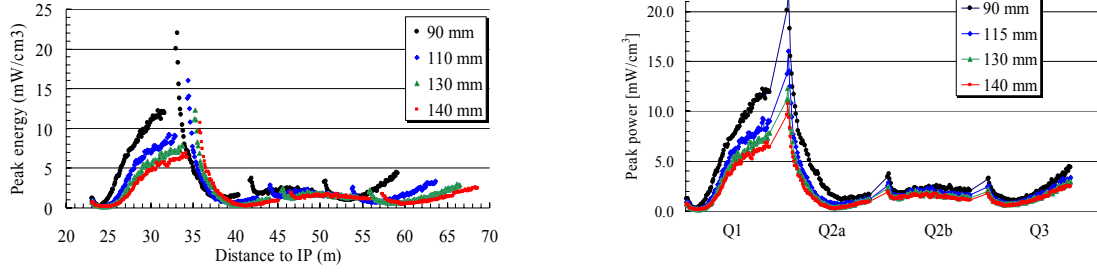


Figure 15: Energy deposition in the magnets depending on the aperture. In the plot on the right each magnet length has been rescaled so that the same length is obtained for different layout cases. There is no additional shielding in Q1.

The main results obtained are shown in Figures 15 and 16 for the luminosity of  $2.5 \cdot 10^{34} \text{ cm}^{-2}\text{s}^{-1}$ . It can be seen from these plots that the energy deposition pattern is similar for all lengths. A longer triplet (increased aperture of the quadrupoles) implies better protection efficiency, as the peak power density decreases with length. Shorter triplets (smaller apertures) have higher energy deposition and may need thicker beam tubes for shielding. The reduction is largest in Q1 and Q2, where the power density is highest. The total heat load in the triplet, including the beam screen, decreases with length (by about 16 % in the range of apertures from 90 to 140 mm). It should be noted that increasing the aperture does not have a big effect on the energy deposition if the field and the layout remain identical. This means that for better protection a thicker beam tube or a local liner is more efficient. In particular, local shielding that shadows the entrance of the downstream magnet is required for reducing the peaks in energy deposition due to the separation between the magnets. These peaks can be seen in Figure 15, in particular between Q1 and Q2. The distribution of particles impinging on the coil is very similar in all cases (about 85 % of photons and 7 % of neutrons). The fluence are inversely proportional to the aperture, for example the peak neutron fluence is  $8.5 \cdot 10^{15} \text{ cm}^{-2}/100 \text{ fb}^{-1}$  for 90 mm aperture and  $5 \cdot 10^{15} \text{ cm}^{-2}/100 \text{ fb}^{-1}$  for 140 mm aperture.

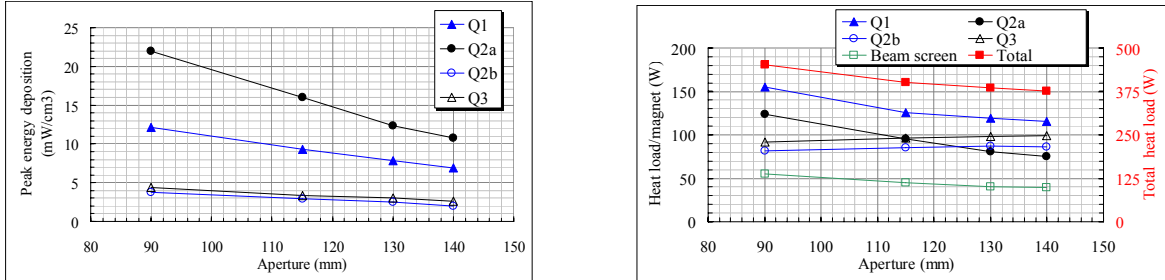


Figure 16: Dependence of the peak power deposited in the triplet quadrupoles on aperture (left), and of the total energy deposited in each magnet and its beam screen (right). The total heat load in the triplet is shown in the plot on the right.

These studies indicate that the peak power density for the luminosity of  $2.5 \cdot 10^{34} \text{ cm}^{-2}\text{s}^{-1}$  is within the design limit for most of the magnets. The peak exceeds the limit of  $4.3 \text{ mW/cm}^3$  only between Q1 and Q2. Fortunately, due to the reduced aperture requirement for Q1, additional shielding can be included as part of the beam screen assembly, effectively eliminating this peak by the shadowing effect. The longitudinal profile of the peak power density in the quadrupole coils is shown in Figure 17 in the case of a 110 mm aperture triplet. This layout was studied in detail and includes a 10 mm thick stainless steel liner in Q1. The results of the parametric study indicate that for the unshielded magnets (i.e. Q2B and Q3) the layout with the preferred 120 mm aperture magnets leads to similar results. Both vertical and horizontal beam crossing schemes were considered (with a half crossing angle of  $225 \text{ } \mu\text{rad}$ ), and the examination of the power density maps indicate that the peaks lie in the crossing plane and change position in the middle of Q2A. The two patterns reflect the different focusing-defocusing action in the crossing plane. For the vertical crossing the maximum appears at the entrance of Q2 and at the end of Q3, followed by a high peak power density in the first corrector. This high value, very sharply localized on the vertical axis, can in principle be decreased by reducing the distance between the triplet and the correctors. Larger aperture of the correctors could also be considered. Local protection inside the interconnections for capturing the debris is also proposed. Further studies are planned to optimize the protection of the correctors.

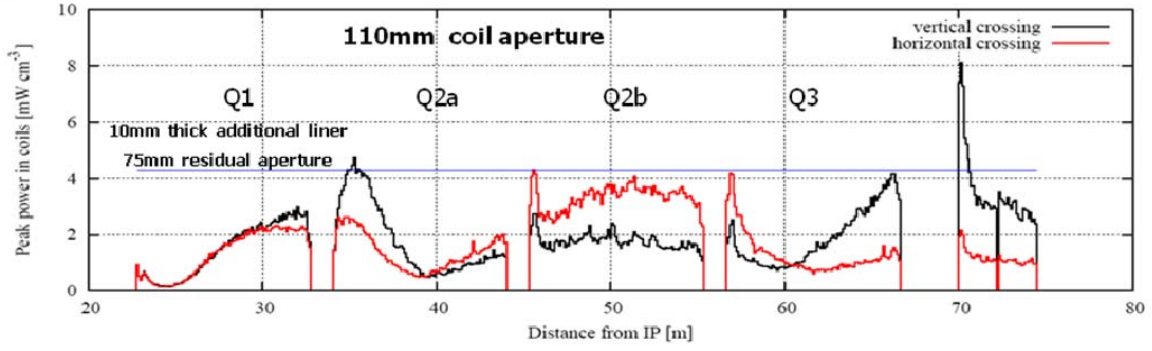


Figure 17: Peak power deposition in the coils of a triplet and correctors with a 110 mm aperture for a luminosity of  $2.5 \cdot 10^{34} \text{ cm}^{-2} \text{ s}^{-1}$ .

The integrated power for the 110 mm aperture triplet is reported in Figure 18, showing the heat load in all magnet components (black) and in the beam screen only (red). In agreement with all other cases, the total heat load in the triplet is about 400 W at 1.9 K, which is still compatible with the existing maximum cooling capacity. In addition, 100 W have to be evacuated by the beam screen (5-20 K), half of which is intercepted by the thick liner in Q1.

The superconducting D1, where an aperture of 180 mm was assumed, is expected to have an additional margin with respect to quench, as the peak power density in its coils is  $1 \text{ mW/cm}^3$ . The total heat load in each of the two modules is about 10-15 W.

An overview of power density in the segment of IR1 and IR5 from the IP up to and including D2 is given in Figures 19 and 20 for the vertical and horizontal beam crossing, respectively. First estimates, not including the TCLP absorber, indicate acceptable values also for the present superconducting D2.

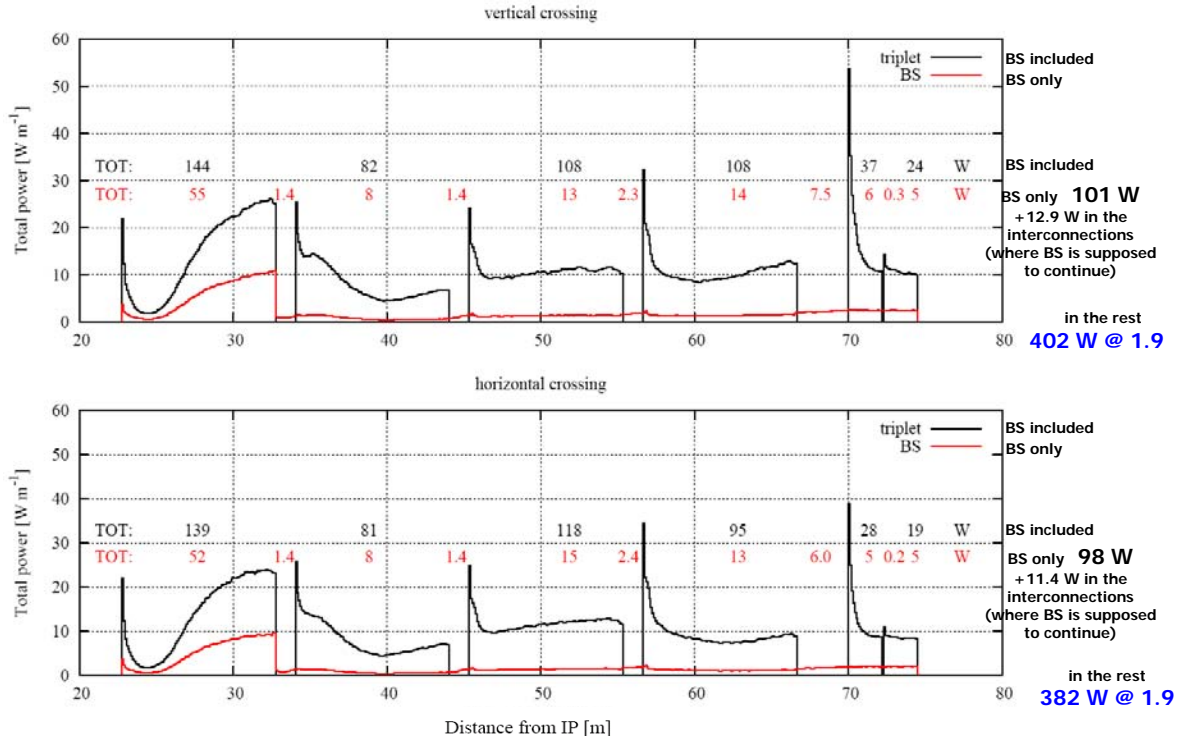


Figure 18: Longitudinal distribution of integrated power and total values for the same layout as in Figure 17.

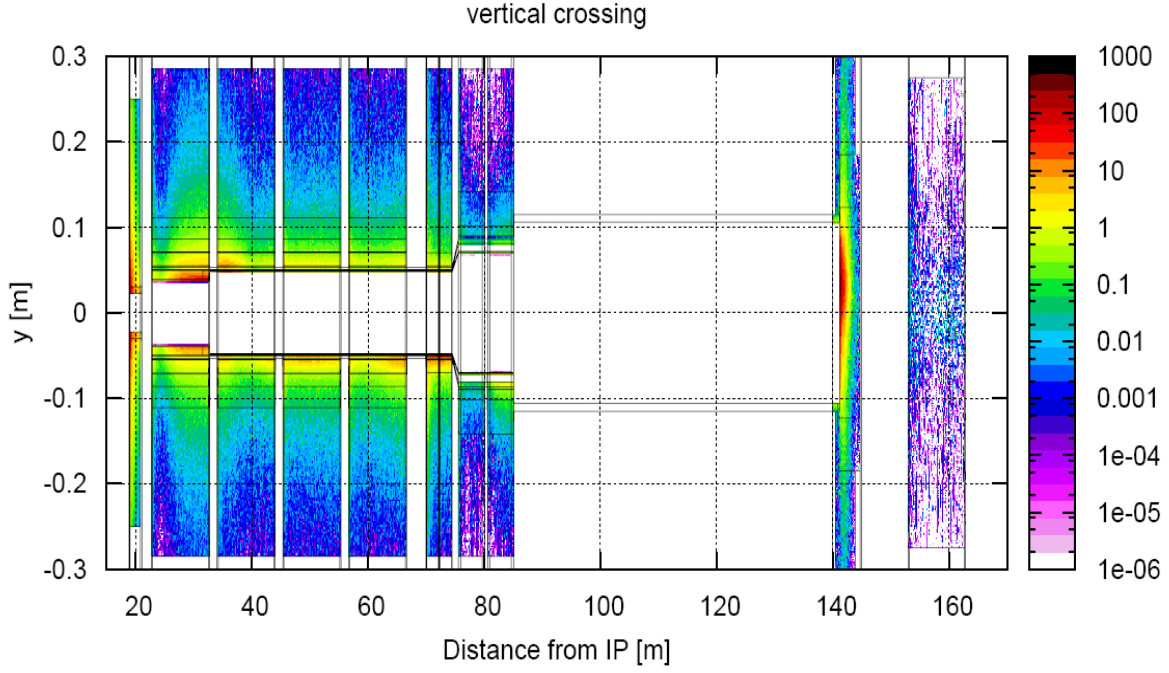


Figure 19: Power density distribution (in  $\text{mW}/\text{cm}^3$ ) in the vertical plane from the TAS to the D2 for vertical beam crossing.

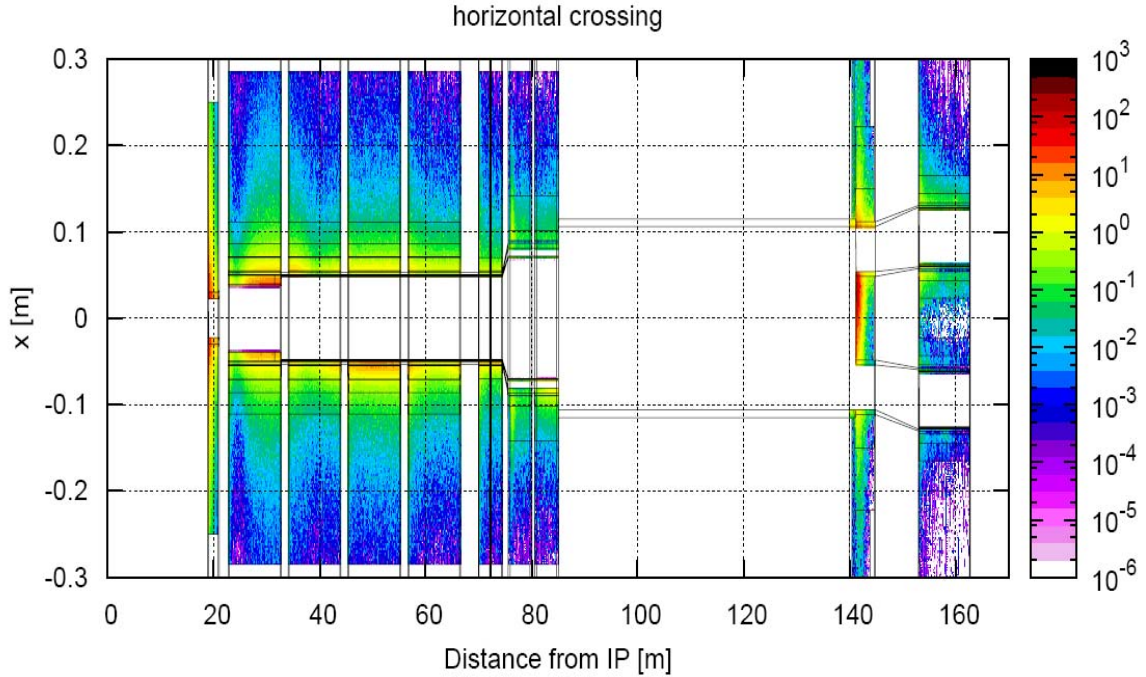


Figure 20: Power density distribution (in  $\text{mW}/\text{cm}^3$ ) in the horizontal plane from the TAS to the D2 for horizontal beam crossing.

## 6.2. Expected dose and equipment lifetime

The debris power in the magnets is also a generator of considerable radiation dose. In the present triplets, a peak dose of 3.5 MGy is expected in the coil for a standard annual run during which  $75 \text{ fb}^{-1}$  of luminosity are accumulated. In the new triplets the dose in the coil inner layer is estimated at about  $2 \text{ MGy}/100 \text{ fb}^{-1}$  but can reach about  $5 \text{ MGy}/100 \text{ fb}^{-1}$  in the innermost strands of the cable. In fact, the dose has a strong azimuthal and radial dependence as shown in Figure 21. For the case of horizontal crossing, the power distribution at

the maximum (middle of Q2B) is given in the left plot, and the corresponding dose values are plotted in the right as a function of radius, averaged over two different azimuthal intervals. With these estimates in mind we have assumed that the magnets and all other equipment for the Phase-I Upgrade must comply with a lifetime of at least  $500 \text{ fb}^{-1}$ . This integrated luminosity is compatible with the lifetime of the ATLAS and CMS experiments before their phase-II upgrade, planned for later in the next decade.

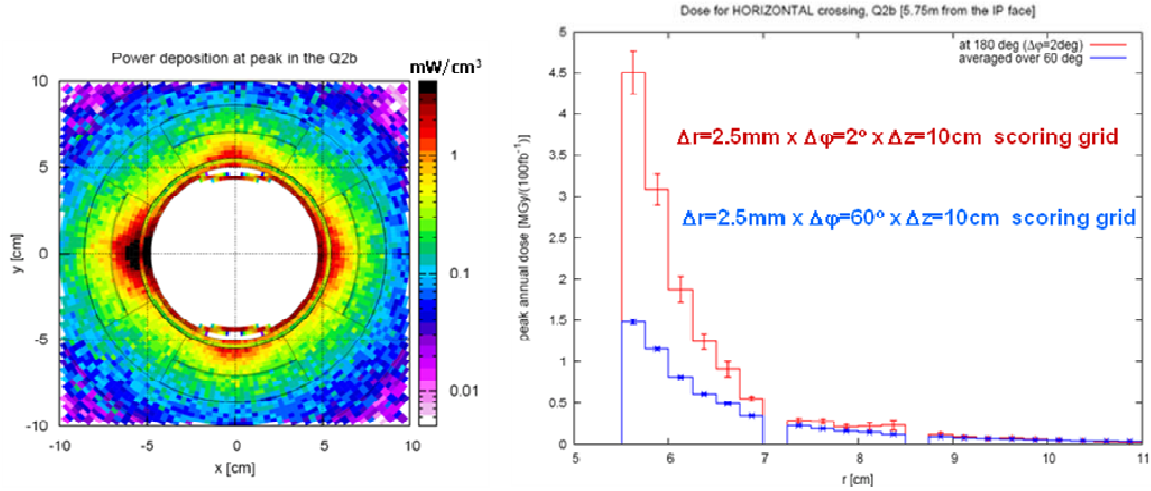


Figure 21: Distribution of power density at the peak (middle of Q2B) (left), and the corresponding radial dose profiles at the peak (negative side of the horizontal axis), averaged over two different azimuthal intervals (right). The plots refer to the horizontal beam crossing.

### 6.3. TAS and TAN absorbers

Very important elements for magnet protection are the two absorbers, TAS and TAN, which already exist in the LHC. The function of these elements remains identical. However, due to the modified magnet apertures and increased luminosity several modifications in their design have to be introduced. The main function of the TAS, located between the border of the experimental area (19 m) and the Q1 quadrupole, is to shield the triplet and reduce backscatter to the experiments. Its vacuum chamber is designed to be as close as possible to the beam envelope. Since the beam size and excursion will increase due to reduced  $\beta^*$ , the vacuum chamber of all four TAS in ATLAS and CMS must be replaced. The most effective way, in terms of access, handling and costs, is to build new TAS bodies and vacuum chambers. This is also an opportunity to introduce a cooling system, as the total heat load in the TAS body with an aperture of 45 mm, compatible with the triplet aperture of 120 mm, will be about 400 W, as indicated in Figure 22, where the longitudinal distribution of integrated power is shown.

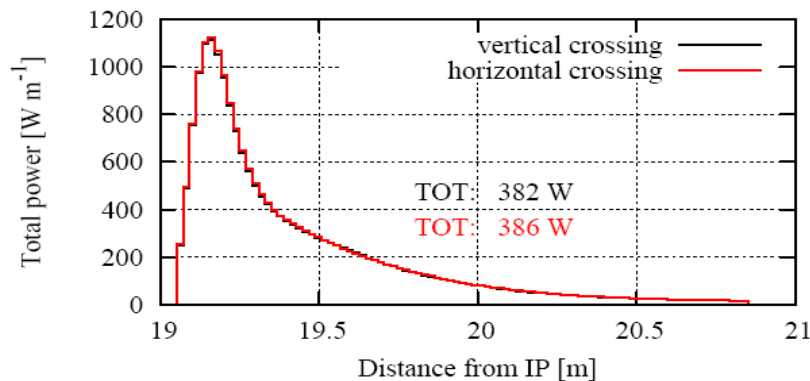


Figure 22: Longitudinal distribution of integrated power and total value for the new TAS (45 mm aperture) for a luminosity of  $2.5 \cdot 10^{34} \text{ cm}^{-2} \text{ s}^{-1}$ .

The TAN is located 140 m from the IP. Its role is to protect all downstream equipment from the neutral particles at the point where the two beams transit from a common to separate vacuum chambers. The present



TAN is perfectly adequate for the luminosity of  $10^{34} \text{ cm}^{-2}\text{s}^{-1}$  and  $\beta^*$  of 0.55 m. However, for a 2.5 times higher luminosity the TAN will receive almost 600 W, as shown in Figure 23. Furthermore, for a  $\beta^*$  approaching 0.25 m, the aperture of the present TAN becomes the limiting element in the insertions. It will therefore need to be considerably modified.

Analyses of the thermo-mechanical stress in the two absorbers and other design issues can be carried out on the basis of the available power deposition maps, like those of Figure 24 where the transverse distribution at the peak in the TAN is shown both for vertical and horizontal beam crossing.

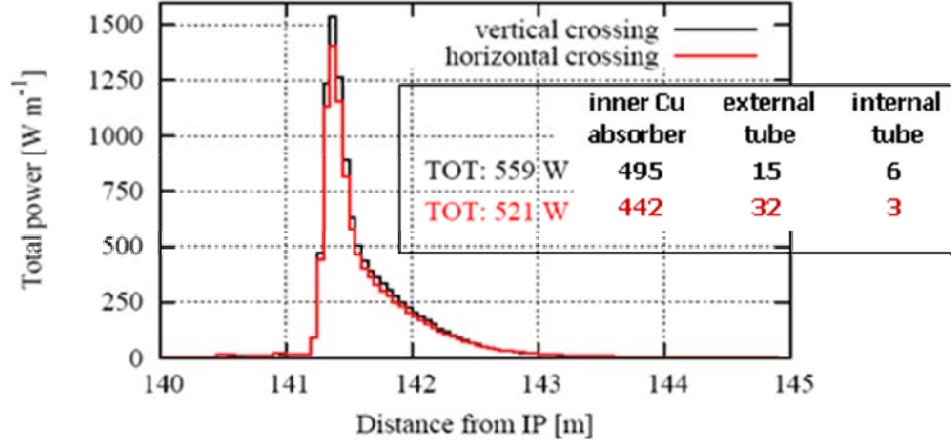


Figure 23: Longitudinal distribution of integrated power and total values for the present TAN for a luminosity of  $2.5 \cdot 10^{34} \text{ cm}^{-2}\text{s}^{-1}$ .

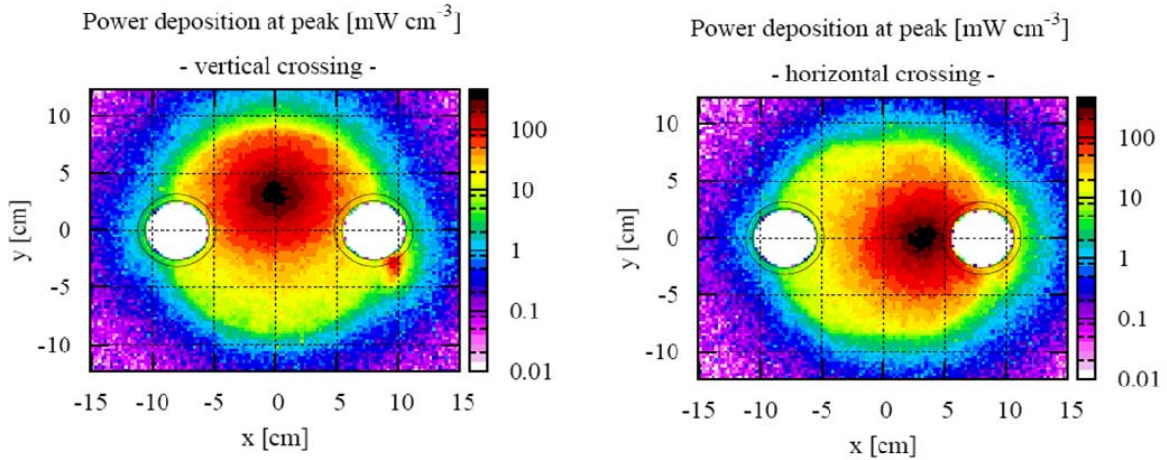


Figure 24: Transverse distribution of power density at the peak in the TAN for vertical (left) and horizontal (right) beam crossing.

#### 6.4. Shielding of equipment areas

A further consequence of high luminosities is the significant level of hadron fluence in the tunnel and in the surrounding areas where electronics equipment will be housed. Following the CNGS run in 2007, which has revealed that high energy ( $>20 \text{ MeV}$ ) hadron fluence above  $10^8 \text{ cm}^{-2}$  may provoke many failures in sensitive electronics due to single event upsets, a campaign has begun at CERN to establish, extend and evaluate the inventory of information needed to assess the risk of radiation-induced electronics failures in the LHC underground areas. Recent estimates indicate that the alcove close to CMS where the electronics of the present triplet is housed (UJ56), is exposed to a fluence of high energy hadrons above  $10^9 \text{ cm}^{-2}/100 \text{ fb}^{-1}$ . Appropriate solutions are being looked at and the fluence levels in other areas of interest are being calculated, including the total dose and 1 MeV equivalent neutron fluence, relevant to surface and lattice displacement damage, respectively.



## 6.5. Radiation protection

The installation of the Phase-I Upgrade magnets entails replacement of the presently installed equipment, which will be highly activated after several years of LHC operation. Interventions in such high radiation areas have to be planned in detail and optimized in terms of the ALARA principle [28]. Optimizing these interventions requires detailed simulations of the residual dose rates with emphasis on the critical areas. The residual dose rates in IR5 for the region from the TAS up to and including the TAN are shown in Figure 25. The simulated area includes all equipment, concrete shielding and the tunnel structure. The residual dose rates in zones A to E are listed in Table 7 for six cooling times, from 1 hour to 4 months. The simulations were performed for an interaction rate of  $5.7 \cdot 10^8$  inelastic interactions per second and 180 days of continuous beam. In order to have a first estimate of the residual dose rates after the Phase-I Upgrade, the results in Table 7 should be multiplied with the ratio of the luminosities (factor of 2 to 3).

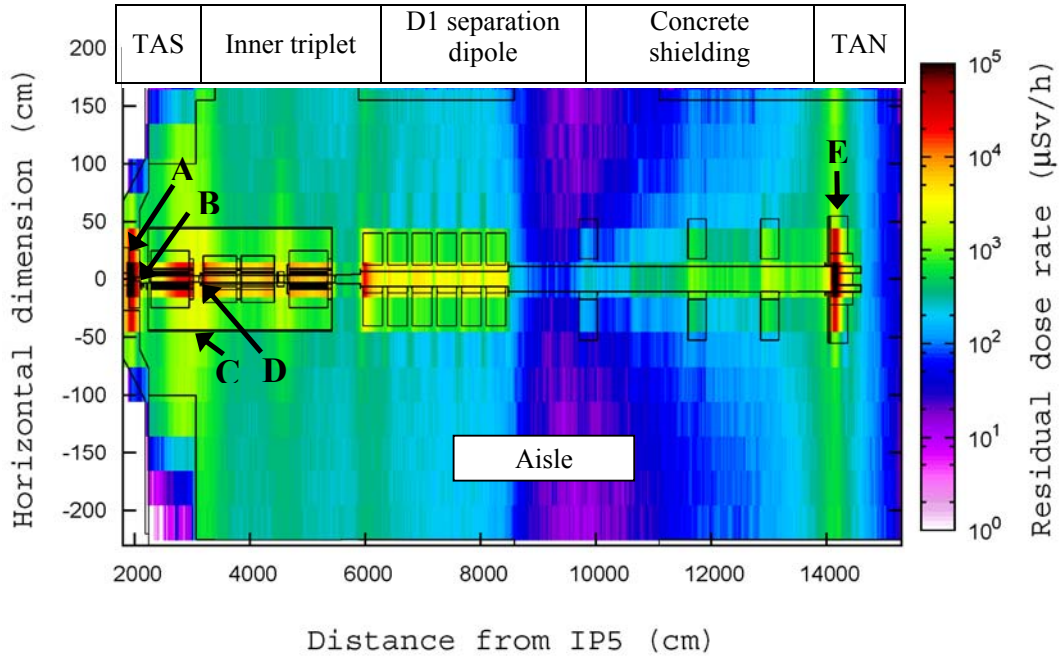


Figure 25: Residual dose rates in IR5 after 180 days continuous LHC operation with  $5.7 \cdot 10^8$  inelastic pp-collisions per second and a cooling time of 1 hour. The geometry contains all major beam line elements between TAS and TAN and the complete tunnel structure.

Table 7: The residual dose rates for the points A to E are listed as function of the cooling time. The simulations were performed for an interaction rate of  $5.7 \cdot 10^8$  inelastic interactions per second and 180 days of continuous beam.

Cooling time	Residual dose rate in (μSv/h)				
	TAS		Triplet		TAN
	A	B	C	D	E
1 hour	2.9E+04	2.0E+03	1.1E+03	3.8E+03	8.4E+02
8 hours	2.0E+04	1.6E+03	8.5E+02	3.0E+03	6.4E+02
1 day	1.4E+04	1.4E+03	6.0E+02	2.6E+03	4.3E+02
1 week	7.3E+03	1.0E+03	2.9E+02	1.6E+03	2.0E+02
1 month	4.6E+03	5.8E+02	1.5E+02	8.4E+02	1.4E+02
4 month	2.4E+03	1.2E+02	7.1E+01	3.5E+02	6.5E+01

From Table 7, it may be seen that the TAS is the most radioactive component. The high residual contact dose rates, even after long cooling times, indicate that remote handling of the TAS in Phase-I should be

implemented. High residual dose rates are also present in the interconnections of the triplet. Due to the limited access, the activities for maintenance and dismantling of the magnets have to be carefully planned. Quick release flanges, or similar solutions, are recommended for these areas. The TAN is also a critical area, especially the copper bars and forward detectors. The radiation dose in the TAN is asymmetrical due to horizontal beam crossing in IR5, which causes a difference of a factor 1.4 in the residual dose rates at the two sides of the TAN.

## 7. Vacuum system

The Phase-I Upgrade will imply redesigning the vacuum systems in a large segment of IR1 and IR5, in particular in the region between D1 and the forward experimental chamber. The most important modifications are expected in the triplets where the elements of the beam vacuum need to comply with the considerably larger aperture of the quadrupoles. A number of modifications will also be made between Q1, TAS and the experimental chambers, where larger apertures and other changes proposed by the experiments are also expected. It is not presently foreseen to modify the vacuum system in the magnets of the matching sections. However, as additional collimators are likely in this region, modifications of the room temperature beam vacuum system in some locations may be required. In the following, further considerations of the triplet vacuum system are given.

### 7.1. Vacuum system in the triplets

The beam vacuum system of the upgraded triplets will consist of a single cold bore at 1.9 K operating temperature. Sector valves will be located at both extremities of the triplets to allow independent interventions on the room temperature and cold vacuum systems.

#### 7.1.1. Beam vacuum requirements

During LHC operation, the beam vacuum is subjected to stimulated desorption induced by photons, electrons, ions and debris coming from the interaction points [4]. Therefore, a significant amount of gas load is condensed on the cryogenic vacuum system. The ionisation of the residual gas by the circulating proton beams induces an ion bombardment of the vacuum chamber, stimulating gas desorption and subsequently further ionisation leading to a pressure runaway. The LHC vacuum system must be designed to avoid such pressure instability. Despite the large diameter of the cold bore tube, the available pumping speed from the extremities of the new triplets will not be sufficient to control the molecular desorption induced by the ion bombardment along the length of the cold bore. A pressure runaway could be reached within a few months of operation. The introduction of a perforated beam screen into the cold bore is therefore required to control the gas density over the full length of the triplets [29].

To be consistent with the LHC baseline design, an average equivalent hydrogen gas density of  $\leq 1.5 \cdot 10^{13} \text{ H}_2/\text{m}^3$  is required in IR1 and IR5. An effective beam screen transparency of  $\sim 5\%$  should be sufficient to maintain the equivalent hydrogen gas density in the new triplets to around  $5 \cdot 10^{14} \text{ H}_2/\text{m}^3$ . This gas density is dominated by the molecular desorption induced by the electron bombardment due to an electron cloud which is expected to dissipate initially about 1 W/m. In such circumstances, the average equivalent hydrogen gas density in the interaction regions is expected to be around  $5 \cdot 10^{13} \text{ H}_2/\text{m}^3$ . In the case of a fully conditioned surface, the electron flux on the surface is reduced and the dissipated power decreases to 20 mW/m, in which case the design gas density is reached [30].

It should be pointed out that the effective beam screen transparency (the pumping speed) depends on the beam screen thickness and the pumping slot width. In the LHC arc beam screen, with 1.1 mm thick wall and 1.5 mm pumping slot width, the effective transparency is roughly half the geometrical transparency.

#### 7.1.2. Beam screens

The beam screen inner surface will be maintained at 7-22 K by means of supercritical He at 5-20 K inside the beam screen cooling tubes. An alternative operating temperature range (40-60 K) is cryogenically less advantageous [18] and therefore not further investigated.

The design heat load on the beam screen is 4 W/m from collision debris, beam screen supports, image currents, electron multipacting and cold to warm transitions (Section 4.3). This heat load can be evacuated with 4 “standard” beam screen cooling tubes (OD 4.76 mm, ID 3.7 mm).

The beam screen manufacture will be based on the technology developed for the baseline LHC beam screens. A high manganese content austenitic stainless steel grade [31] will provide low magnetic permeability ( $<1.005$  at 4.2 K) and mechanical strength to withstand magnet quenches. A high purity grade (OFE) inner copper layer will provide low impedance and suitable vacuum properties. The gas density inside

the beam screen will be controlled by means of 16 rows of pumping slots whose size and geometry will be optimised to obtain sufficient pumping speed. The baseline beam screen support system, which mechanically supports and thermally insulates the beam screen from the cold bore at 1.9 K, will have to be adapted to the larger diameter and increased weight of the new beam screens. In particular the Q1 beam screen with its integrated absorber will most likely weigh over 15 kg/m.

In order to reduce the design and manufacturing costs, the beam screens for the new triplets will preferably be of identical design, accommodating both horizontal and vertical beam crossing schemes. Beam screen cross sections under consideration are shown in Figure 25. The 120 mm aperture cryo-magnets will be equipped with a cold bore with an inner diameter of around 110 mm. Taking into account the expected manufacturing tolerances [32], a half-aperture (at operating conditions) of 49 mm in the beam screen corners (A1) and 44 mm between flats (A2) should be feasible. Further calculations will allow optimising the beam screen wall thickness and aperture.

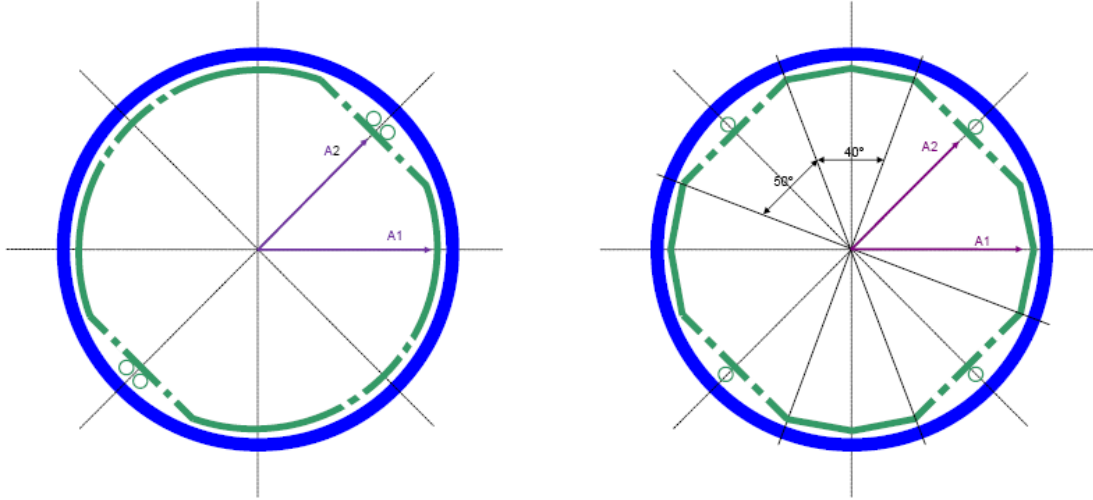


Figure 25: Beam screen cross sections under consideration.

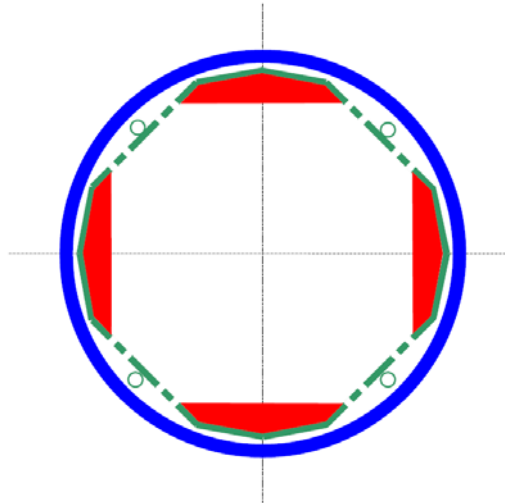


Figure 26: Possible cross section of Q1 beam screen with integrated absorber.

The Q1 beam screen will be equipped with an absorber to intercept part of the heat load from particle debris generated during collisions. The heat load intercepted by the Q1 beam screen will depend on the absorber thickness and material density. Positioning the absorber inside the Q1 beam screen will allow using the same beam screen cross section along the triplets. The absorber should not obstruct the pumping slots and has to be thermalized to the beam screen cooling tubes. Its geometry and thickness will be optimised with

respect to the manufacturing costs and aperture. Absorber geometry under consideration is shown in Figure 26.

### **7.1.3. Beam vacuum interconnects**

The beam vacuum interconnects will be based on the present LHC design with a plug-in module ensuring low impedance and accommodating thermal movements during cool-down and warm-up [4]. Cold-to-warm transitions will be mounted at the triplet extremities. Their design will be extrapolated from the existing solutions.

### **7.1.4. Insulation vacuum system**

The insulation vacuum system (pumps, gauges, pumping ports, overpressure valves, etc.) for the upgraded triplet cryo-magnets will be identical to the current system.

## **8. Triplet alignment system**

It is assumed that the alignment requirements for the upgrade are similar to the present LHC triplets. The expected relative alignment accuracy of one triplet with respect to the magnets in the corresponding arcs and matching sections should therefore be  $\pm 0.1$  mm (rms), both in radial and vertical directions. The same alignment accuracy is expected between the two triplets across IP1 and IP5. The stability of each low- $\beta$  quadrupole is expected to be a few  $\mu\text{m}$ , while the control of their position will be done with a resolution of a few  $\mu\text{m}$ . This section details the alignment functions, as well as the improvements foreseen.

### **8.1. Metrology of the assembled cryo-magnets**

The determination of the coordinates of the fiducials, located on the cryo-magnets, with respect to the as-built mechanical and magnetic axis of the quadrupole is the basic information necessary for all further alignment actions. On the present triplets, this measurement was carried out in warm and cold conditions at Fermilab, initially with a simple control at CERN. As the results showed changes of the fiducialization during ocean-going transport, the metrology of the quadrupoles was redone at warm using the tools and techniques developed for the LHC cryo-magnets. In the case of the triplets for Phase-I Upgrade, all warm and cold measurements (both magnetic and geometric) will be performed at CERN using the existing LHC test benches, measurement tools and procedures that are well understood. The following improvements of the magnet metrology should be further implemented:

- The straightness of the cold mass and the position of the vacuum pipe should be controlled during the manufacturing phase of the cold mass.
- The supporting system of the cold mass and the transport restraints for the magnet should guarantee that there is no displacement of the cold masses inside the cryostat during transport to the tunnel. For this purpose, a dedicated system for monitoring the displacements of the cold masses should be installed.
- Additional reference points on the cold mass extremities increase redundancy and allow to re-fiducialize the magnets in-situ, if needed, and to perform additional geometrical controls of the interconnections areas. These points should be referenced to the beam tubes during final magnet assembly.
- The positions of the fiducial targets on the cryostats, and of the interface points with the jacks, should be measured and re-adjusted if needed after magnet assembly, to allow full flexibility of the alignment system.

### **8.2. Initial alignment**

During installation, the triplet is aligned twice. As a first step, the triplet is aligned with respect to the geodetic network. Once the interconnections and cool-down of the quadrupoles are completed, the triplet alignment is smoothed with respect to the arc and matching section, which provides relative alignment accuracy in vertical and radial directions of  $\pm 0.1$  mm (rms). The methods used for the alignment of the present triplets (measurement of offset to a wire and levelling) proved to be efficient, but must be optimized to satisfy ALARA requirements. Additional space for line-of-sight and for easier access to the triplet must also be made available, especially if shielding is installed around the triplet.

Before the present triplet is dismantled, the local geodetic network will have to be consolidated, in order to have a precise record of the good geometry and co-linearity of the triplet, and to be able to apply them to the new triplet after installation.

### 8.3. Final alignment and stability

Due to high radiation doses and stringent alignment tolerances, alignment systems and motorized jacks must be installed to meet the requirements for the triplet stability. The alignment systems also provide information for the final alignment of the triplets with respect to each other and give permanent tunnel references for the experiments. These systems should be installed before the final triplet tests, in order to monitor the behaviour of the magnets under vacuum, during pressure tests and cool-down.

#### 8.3.1. Alignment systems

Two alignment systems, HLS system (Hydrostatic Levelling System) based on the principle of the communicating vessels, and WPS (Wire Positioning System) based on offset wire measurements, are presently installed in IR1 and IR5 and record five degrees of freedom. The configuration of the systems provides redundancy, which must be kept as it allows control of the sensors. The system as foreseen for the new triplet is shown in Figure 27 and will also include monitoring of the longitudinal axis of each quadrupole.

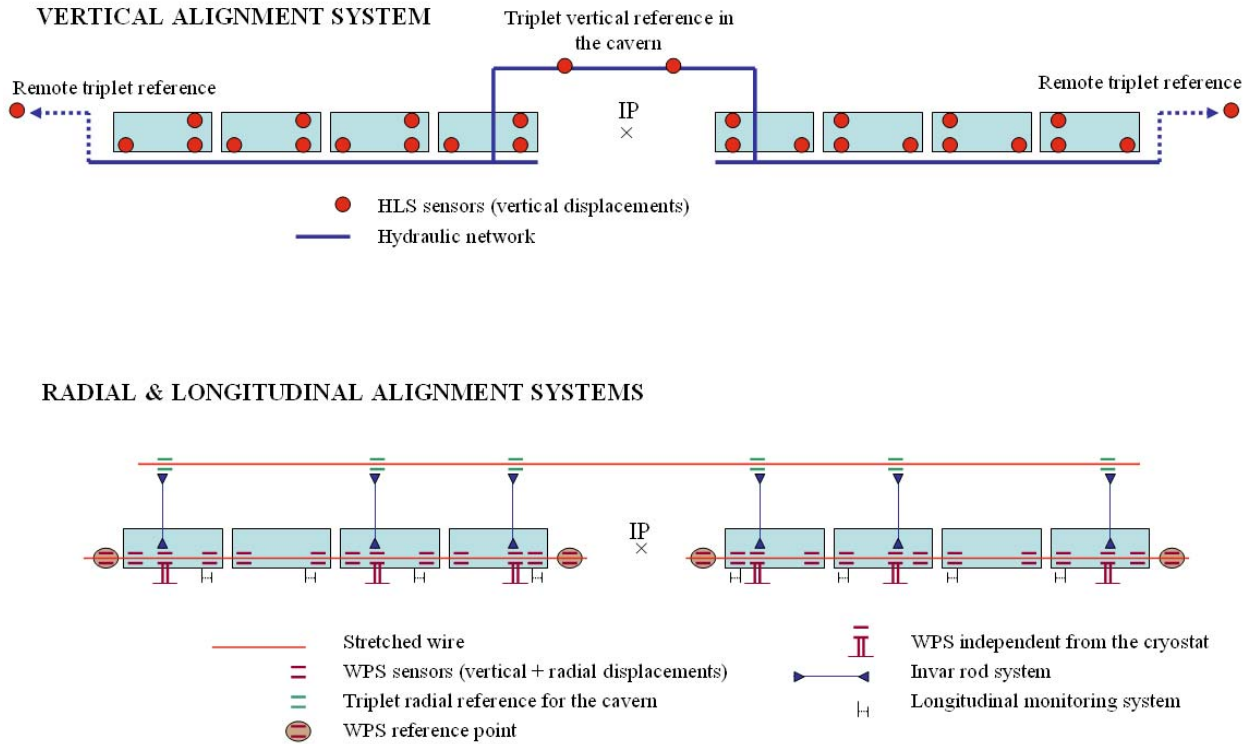


Figure 27: Schematic of the triplet alignment systems in LHC Points 1 and 5.

The link between the two triplets through the UPS galleries must be kept in order to guarantee their co-linearity. For this purpose, additional fiducials, mounted either on pillars or directly on the cryostats depending on the final layout, will be needed for linking the LHC tunnel to the UPS galleries using the existing boreholes, as well as for linking the triplet to the matching sections. The UPS galleries will also serve for the remote electronics of the sensors. Due to limited access to the triplet during normal LHC shutdowns, an extension of the triplet HLS network in the matching sections is necessary.

#### 8.3.2. Motorized jacks

The present LHC triplet is mounted on standard LHC jacks that were slightly modified to allow their motorisation (with a range of  $\pm 2\text{mm}$  and displacement resolution of a few  $\mu\text{m}$ ). It is foreseen that a similar system is used for the triplets in the Phase-I Upgrade. The specification of the jacks will be made once the details of the interconnections are known, in particular the way that internal and external forces are transferred to the ground in all testing and operational situations. Ideally, the forces should not be transmitted

from one cryostat to the other (e.g. via tie-rods, as in the present triplet), and the interconnections should allow quadrupole displacement of  $\pm 2$  mm in all directions in operating conditions.

## 9. Tunnel integration

As mentioned, the power converters and quench protection equipment for the present triplets are housed in the alcoves, while the feed-boxes and cryogenic instrumentation are in-line with the triplet or below the cryostats. Unfortunately, the equipment layout around ATLAS and CMS is not identical. In fact, the location of equipment alcoves is symmetric in ATLAS (UJ14 and UJ16), Figure 28, while they are quite different one from the other in CMS (USC55 and UJ56), Figure 30. The cross-section of the beam tunnels in the two IRs is also different. This has led to a situation where the design of the present feed-boxes and the detailed layout of the equipment are different for all triplets in the LHC. The design goal for the Phase-I Upgrade is to have identical feed-boxes for the four new triplets. Other equipment, in particular the exact routing of the superconducting links, will have to be adapted to the local situation.

The available space in the UJ alcoves and USC is shared with other machine equipment and is almost fully occupied. Nevertheless, in reviewing the situation it has been possible to identify possible locations for the new power converters, feed-boxes and protection equipment racks. In case of ATLAS, the space that could be used is the ground and first floors of the UJ caverns, as shown in Figure 29. However, radiation level in these areas is expected to be high (Section 6.4). Alternatively, radiation sensitive equipment could be located in the UL14 and UL16 passageways, as well as in the US15 cavern. The situation in CMS is more difficult, and at present the most promising solution is to place the equipment in the UL54 and UL56 by-passes, as shown in Figure 31. In both cases, additional studies are necessary to find the appropriate solutions for routing the superconducting links while keeping most of the equipment in low radiation areas. Minimal civil engineering may still be necessary.

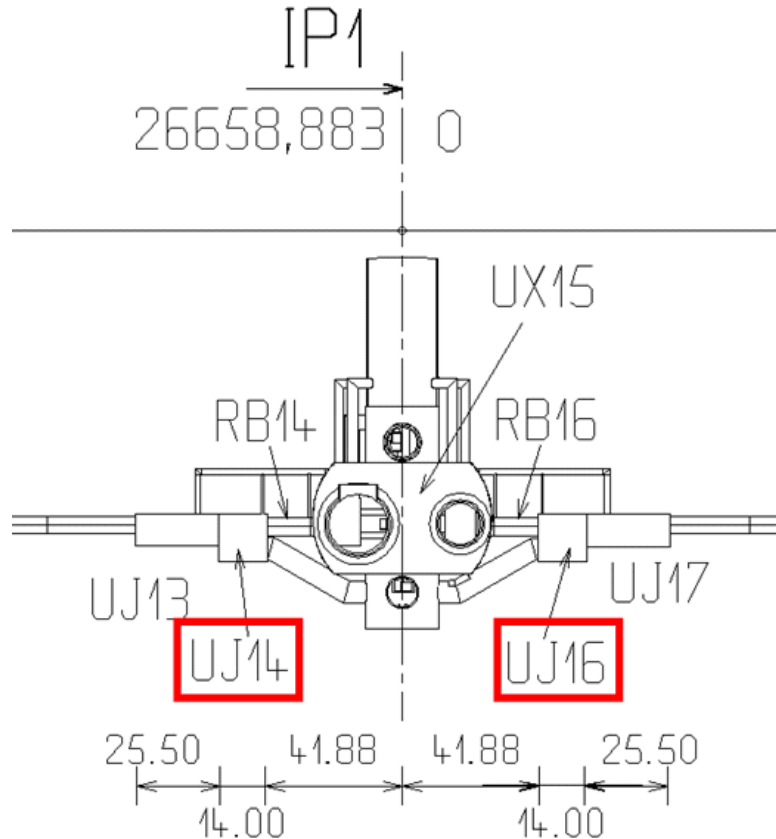


Figure 28: LHC tunnel (RB14 and RB16) and equipment alcoves (UJ14 and UJ16) around the ATLAS (UX15) cavern.

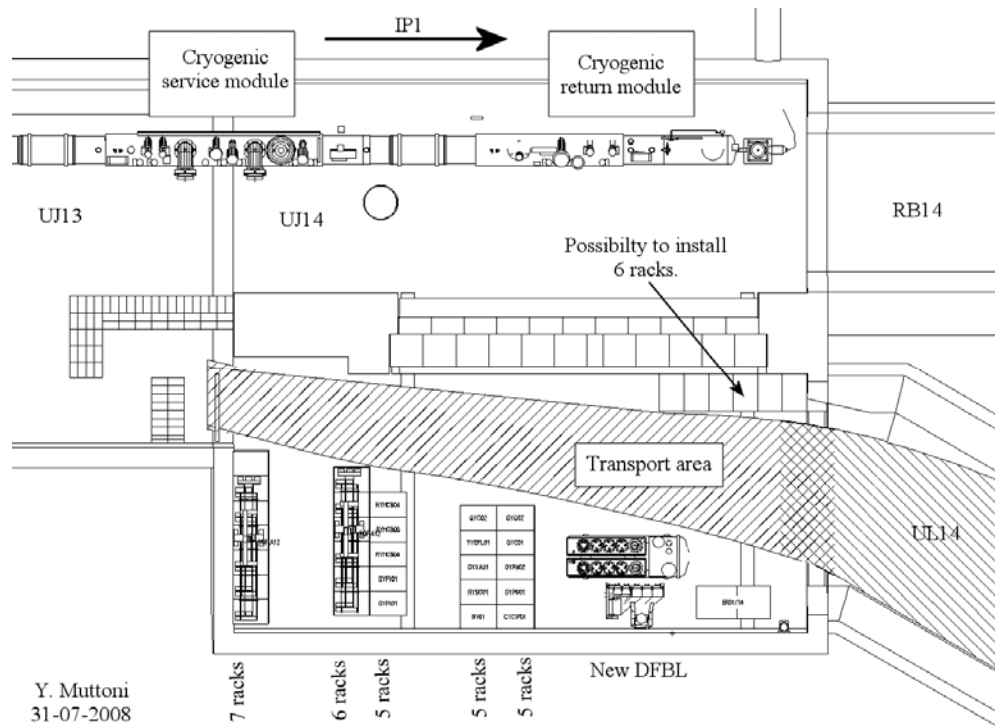


Figure 29: A first study of the layout of the current lead box, power converters and protection electronic racks in the ground floor of UJ14. Radiation sensitive equipment should be placed in UL14 and US15 (not shown in the plot). Transport area must be kept clear.

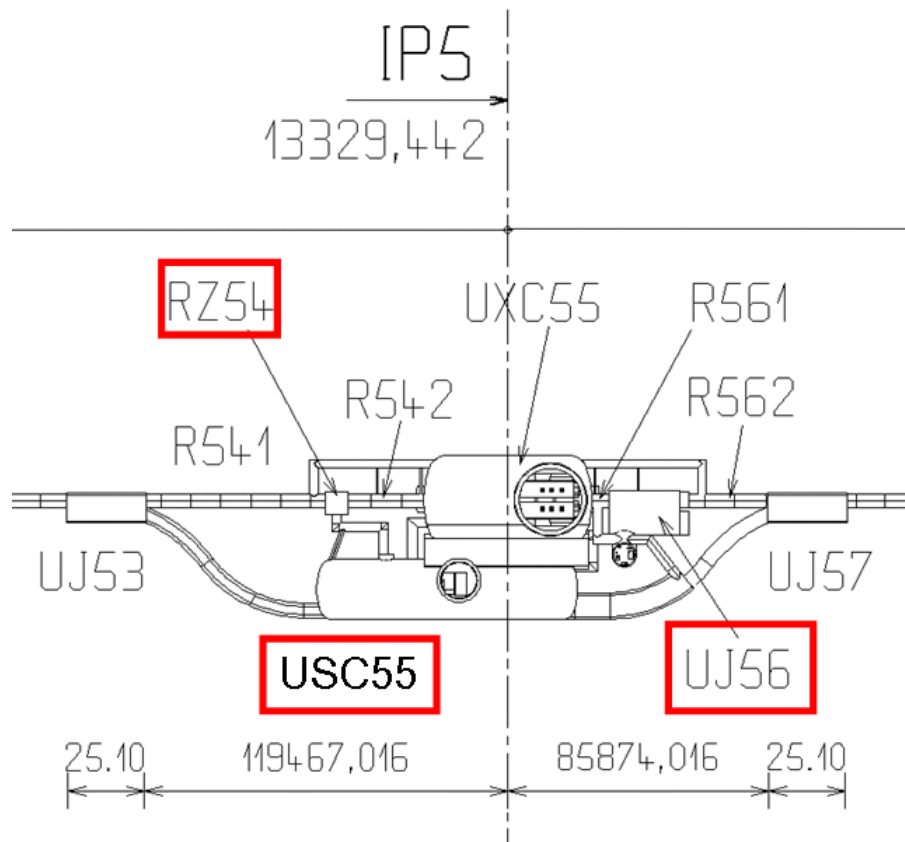


Figure 30: LHC tunnel (R542 and R561) and equipment alcoves (USC55 and UJ56) around the CMS (UXC55) cavern.

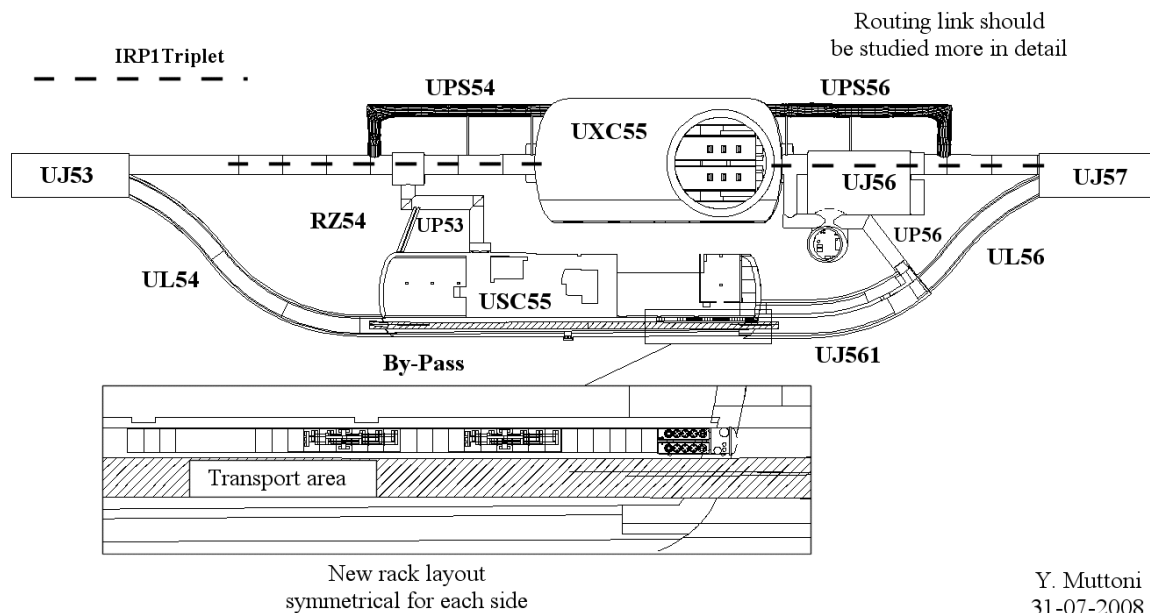


Figure 31: A first study of the layout of the current lead box, power converters and protection electronic racks in the UL54 and UL56 by-passes around CMS cavern. Transport area must be kept clear.

## 10. Project organization and planning

The Phase-I Upgrade is organized as a CERN project since the beginning of 2008. In this framework, the work-packages have been defined with clear technical goals and milestones. Project engineers have been assigned and preliminary estimates of the necessary resources and costs have been made. The quality assurance of the technical specifications and change control will use the EDMS system developed for the LHC.

The project plan foresees that the production of the low- $\beta$  quadrupoles, their cryostating and cold testing is performed in CERN workshops and testing facilities. Nonetheless, to profit from the engineering expertise in other institutions, CERN has invited European and US laboratories to contribute significantly to the Phase-I Upgrade. As a result, as part of the “SLHC-Preparatory Phase” project (CNI, 7<sup>th</sup> EU Framework Programme), other European laboratories (CEA and CNRS-France, CIEMAT-Spain, STFC-UK) are participating in the design of the quadrupoles, correctors and associated production tooling. Furthermore, within the special French contribution to the implementation of the European strategy for particle physics (“White paper”), a considerable participation of CEA and CNRS is foreseen in providing the components for magnets and cryostats and manufacture of the correctors. These collaborations are well under way, with formal agreements already signed and in effect. It is also expected that the US laboratories, which have contributed decisively to the construction of the present LHC triplets, will participate in the LHC upgrade, both phase-I and phase-II. Discussions with the US laboratories are ongoing and it is expected that for the Phase-I Upgrade they will provide the D1 magnets and a significant part of the cold power transfer system.

In parallel with the activities on project organization, discussions were held in the LHC IR Upgrade Working Group to update and clarify the input and prepare technical alternatives. This work has also relied on information discussed in conferences and workshops, in particular those organized by CARE. The present Report completes the first major milestone of the Project, and summarizes the decisions taken in the conceptual design review [33]. It will be followed by the technical design report, foreseen to be completed in mid-2009. Later the same year, results from model magnet tests should be available. The production of the quadrupoles and other magnets is planned for 2010-2012. An important milestone is the string test foreseen in 2012 that should resolve any outstanding issue and minimize the commissioning time of the new magnets in the tunnel environment.

The implementation of the upgrade is presently foreseen for the first half of 2013. A preliminary planning exercise [34] has shown that the removal of the present triplets in the ATLAS and CMS interaction regions and the installation of the new triplets and all other equipment could be achieved in a six month period. A



similar duration has also been found necessary for the final phase of Linac4 commissioning. During that time, the proton injector chain will not be available and a CERN-wide shutdown and maintenance period is foreseen. ATLAS and CMS are also planning substantial modifications during this period to prepare for higher event rates. All these activities will need considerable CERN-wide coordination and scheduling.

## 11. References

- [1] The European strategy for particle physics, CERN/2685.
- [2] R. Garoby, "Upgrade Issues for the CERN Accelerator Complex", Proc. EPAC'08, Genoa, Italy (2008), p.3734.
- [3] R. Ostojic et al, "The Construction of the Low-Beta Triplets for the LHC", Proc. PAC'05, Knoxville, TN (2005), p.2798.
- [4] LHC Design Report, CERN-2004-003.
- [5] R. Assmann, LHC IR Upgrade Working Group, LIUWG-4, 11 Nov 2007, <http://liuwg.web.cern.ch/liuwg..>
- [6] S. Fartoukh, LHC IR Upgrade Working Group, LIUWG-15, 28 May 2008, <http://liuwg.web.cern.ch/liuwg>.
- [7] W. Herr, LHC IR Upgrade Conceptual Design Review, 31 July 2008, <http://indico.cern.ch/conferenceDisplay.py?confId=36286>
- [8] D. Tommasini, D. Richter, "New Cable Insulation Scheme Improving Heat Transfer to Superfluid Helium in Nb-Ti Superconducting Accelerator Magnets", Proc. EPAC'08, Genoa, Italy (2008), p.2467.
- [9] F. Borgnolutti, E. Todesco, A. Mailfert, "130 mm Aperture Quadrupoles for the LHC Luminosity Upgrade", Proc. PAC'07, Albuquerque, USA (2007), p. 351.
- [10] N. Schwerg, LHC IR Upgrade Working Group, LIUWG-17, 17 July 2008, <http://liuwg.web.cern.ch/liuwg>.
- [11] F. Regis, LHC IR Upgrade Working Group, LIUWG-14, 15 May 2008, <http://liuwg.web.cern.ch/liuwg>.
- [12] M. Anarella et al., "The RHIC Magnet System", NIM A499 (2003) 280-315.
- [13] G. Riddone, L. Tavian, R. van Weelderen, "Dimensions, Pressures, Temperatures and Valve Sizing in Machine Cryostat and Cryogenic Distribution Line for the LHC", LHC Project Note 135, 1998-03-06.
- [14] Heat Load Working Group, "Heat Load Assessment", <http://lhc-mgt-hlwg.web.cern.ch/lhc-mgt-hlwg/HLWG/ASSESSMENT/HLassessment.htm>.
- [15] D. Weiss, H.C. Hseuh, BNL Memorandum "DX & DX-D0 Beamtube Geometry and Machine Interfaces", October 2, 1997.
- [16] Ph. Lebrun, L. Serio, L. Tavian, R. van Weelderen, "Cooling Strings of Superconducting Devices below 2 K: The Helium II Bayonet Heat Exchanger", Adv. Cryog. Eng., A: 43 (1998) pp. 419-426.
- [17] B. Rousset, P. Thibault, S. Perraud, L. Puech, P.E. Wolf, R. Van Weelderen, "Heat Transfer Enhancement of He II Co-current Two-phase Flow in the Presence of Atomisation", Proc. 20 ICEC, Beijing, China, 11-14 May 2004, pp.761-764.
- [18] R. Van Weelderen, LHC IR Upgrade Working Group, LIUWG-16, 5 May 2008, <http://liuwg.web.cern.ch/liuwg>.
- [19] A. Ballarino, K. H. Meß and T. Taylor, "Extending the Use of HTS to Feeders in Superconducting Magnets System", IEEE Trans. Appl. Supercond., Vol.18, No. 2, June 2008.
- [20] A. Ballarino, T. Taylor, "Design Concept of a Cold Power Transfer System for the Phase-I Upgrade of the LHC Luminosity Insertions", EDMS No. 965303.
- [21] A. Ballarino, S. Berta, S. Brisigotti, A. Tumino, D. Pietranera, R. Penco, G. Grasso, "Development of MgB2 Conductors for Application to Superconducting Bus", EDMS No. 965302.
- [22] N. Mokhov et al, "Protecting LHC IP1/IP5 Components against Radiation Resulting from Colliding Beam Interactions", LHC Project Report 633, Apr 2003.
- [23] J.P. Koutchouk, L. Rossi, and E. Todesco, "A Solution for Phase-one Upgrade of the LHC Low-beta Quadrupoles Based on Nb-Ti", LHC Project Report 1000 (2007).
- [24] E. Wildner, F. Borgnolutti, F. Cerutti, M. Mauri, A. Mereghetti, E. Todesco, "Parametric Study of Energy Deposition in the LHC Inner Triplet for the Phase-I Upgrade", LHC Project Report 1127 (2008).
- [25] A. Ferrari, P.R. Sala, A. Fasso', and J. Ranft, "FLUKA: a Multi-Particle Transport Code", CERN 2005-10 (2005), INFN/TC\_05/11, SLAC-R-773.
- [26] G. Battistoni, S. Muraro, P.R. Sala, F. Cerutti, A. Ferrari, S. Roesler, A. Fasso', J. Ranft, "The FLUKA Code: Description and Benchmarking", Proc. of the Hadronic Shower Simulation Workshop 2006, Fermilab 6-8 Sep 2006, AIP Conference Proceeding 896, 31-49 (2007).
- [27] S. Roesler, R. Engel, J. Ranft, "The Monte Carlo Event Generator DPMJET-III", Proc. Monte Carlo-2000, Lisbon, 23-26 Oct. 2000, Springer-Verlag Berlin, 1033-1038 (2001).
- [28] Radiation Safety Manual, Safety Code F, CERN, EDMS 33579, (2006).
- [29] V. Baglin, LHC IR Upgrade Working Group, LIUWG-1, 27 Sep 07, <http://liuwg.web.cern.ch/liuwg>.
- [30] V. Baglin, LHC IR Upgrade Working Group, LIUWG-2, 18 Oct 07, <http://liuwg.web.cern.ch/liuwg>.
- [31] S. Sgobba and G. Hochörtler, Int. Conf. Stainless Steel '99, Chia Laguna, Italy, 6-9 June 1999.
- [32] N. Kos, LHC IR Upgrade Working Group, LIUWG-14, 15 May 2008, <http://liuwg.web.cern.ch/liuwg>.
- [33] LHC IR Upgrade Conceptual Design Review, 31 July 2008, <http://indico.cern.ch/conferenceDisplay.py?confId=36286>
- [34] K. Foraz, LHC IR Upgrade Conceptual Design Review, 31 July 2008, <http://indico.cern.ch/conferenceDisplay.py?confId=36286>